REPORT NO. NADC-80094-60

LEVEL II

12 B.S.

AD A093953

PREDICTION AND EVALUATION OF THRUST AUGMENTING EJECTOR PERFORMANCE AT THE CONCEPTUAL DESIGN STAGE

K. A. Green
Aircraft and Crew Systems Technology Directorate
NAVAL AIR DEVELOPMENT CENTER
Warminster, Pennsylvania 18974

30 APRIL 1980

FINAL REPORT
TASK AREA NO. WF41400000
WORK UNIT NO. AZ602

APPROVED FOR PUBLIC RELEASE; DISTRIBUTION UNLIMITED

Prepared for
NAVAL AIR SYSTEMS COMMAND
Department of the Navy
Washington, D.C. 20361

NADC-80094-60

N O T I C E S

REPORT NUMBERING SYSTEM - The numbering of technical project reports issued by the Naval Air Development Center is arranged for specific identification purposes. Each number consists of the Center acronym, the calendar year in which the number was assigned, the sequence number of the report within the specific calendar year, and the official 2-digit correspondence code of the Command Office or the Functional Directorate responsible for the report. For example: Report No. NADC-78015-20 indicates the fifteenth Center report for the year 1978, and prepared by the Systems Directorate. The numerical codes are as follows:

CODE	OFFICE OR DIRECTORATE
00	Commander, Naval Air Development Center
01	Technical Director, Naval Air Development Center
02	Comptroller
10	Directorate Command Projects
20	Systems Directorate
30	Sensors & Avionics Technology Directorate
40	Communication & Navigation Technology Directorate
50	Software Computer Directorate
60	Aircraft & Crew Systems Technology Directorate
70	Planning Assessment Resources
80	Engineering Support Group

PRODUCT ENDORSEMENT - The discussion or instructions concerning commercial products herein do not constitute an endorsement by the Government nor do they convey or imply the license or right to use such products.

APPROVED BY: _____ DATE: 10/8/80

E. J. STURM
CDR USN

UNCLASSIFIED

SECURITY CLASSIFICATION OF THIS PAGE (When Data Entered)

REPORT DOCUMENTATION PAGE

READ INSTRUCTIONS BEFORE COMPLETING FORM

1. REPORT NUMBER: NADC-80094-60	2. GOVT ACCESSION NO.: AD-A093953
3. RECIPIENT'S CATALOG NUMBER:	
4. TITLE (and Subtitle): Prediction and Evaluation of Thrust Augmenting Ejector Performance at the Conceptual Design Stage.	5. TYPE OF REPORT & PERIOD COVERED: Final Report. Oct 78 - Sep 79
	6. PERFORMING ORG. REPORT NUMBER:
7. AUTHOR(s): K. A. Green	8. CONTRACT OR GRANT NUMBER(s): F41400
9. PERFORMING ORGANIZATION NAME AND ADDRESS: Naval Air Development Center, Warminster, PA 18974	10. PROGRAM ELEMENT, PROJECT, TASK AREA & WORK UNIT NUMBERS: P.E. 62241N W.U. No. ZA602; Proj. F41400; A.T. WF41400000
11. CONTROLLING OFFICE NAME AND ADDRESS: Naval Air Systems Command, Jefferson Plaza, Washington, DC 20361 (AIR-320D)	12. REPORT DATE: 30 Apr 80
	13. NUMBER OF PAGES: 48
14. MONITORING AGENCY NAME & ADDRESS (if different from Controlling Office)	15. SECURITY CLASS. (of this report): UNCLASSIFIED
	15a. DECLASSIFICATION/DOWNGRADING SCHEDULE

16. DISTRIBUTION STATEMENT (of this Report)

Approved for Public Release; Distribution Unlimited

17. DISTRIBUTION STATEMENT (of the abstract entered in Block 20, if different from Report)

18. SUPPLEMENTARY NOTES

19. KEY WORDS (Continue on reverse side if necessary and identify by block number)

VTOL
Ejector
Augmenter

20. ABSTRACT (Continue on reverse side if necessary and identify by block number)

The performance characteristics of thrust augmenting ejectors, based on a computerized one-dimensional analysis technique, are shown. Various loss mechanisms within the ejector are described and the sensitivity of the ejector performance to these loss mechanisms are illustrated. Performance estimates have been made for several ejector configurations for which experimental data are available. Despite the assumptions that have to be made, in order that the problem be tractable for the one dimensional analysis, good agreement

DD FORM 1 JAN 73 1473 EDITION OF 1 NOV 65 IS OBSOLETE S/N 0102-LF-014-6601

UNCLASSIFIED

SECURITY CLASSIFICATION OF THIS PAGE (When Data Entered)

393532

between the predicted and experimental values have been obtained. Other more complex (2 D and 3 D) codes have also been examined but were found to be expensive to run and in some cases limited in application.

FORWARD

This document describes the estimation of thrust augmenting ejector performance for use as a tool at the conceptual design stage. The work was performed during the period October 1978 to September 1979 and was sponsored by Mr. R. Siewert (AIR-320D) of the Naval Air Systems Command under AIRTASK A03V/-0C00/001B/WF41-400-000.

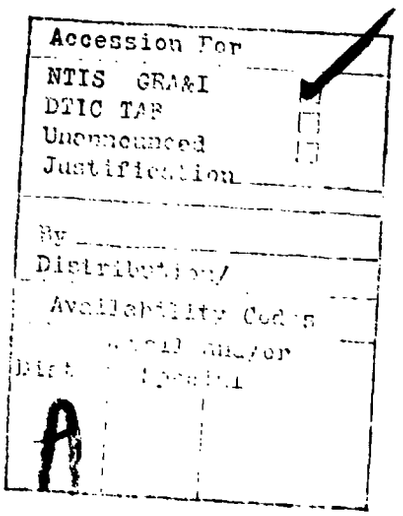

SUMMARY

The performance characteristics of thrust augmenting ejectors, based on a computerized one-dimensional analysis technique, are shown. Various loss mechanisms within the ejector are described and the sensitivity of the ejector performance to these loss mechanisms are illustrated. Performance estimates have been made for several ejector configurations for which experimental data are available. Despite the assumptions that have to be made, in order that the problem be tractable for the one dimensional analysis, good agreement between the predicted and experimental values have been obtained. Other more complex (2 D and 3 D) codes have also been examined but were found to be expensive to run and in some cases limited in application.

TABLE OF CONTENTS

LIST OF FIGURES

LIST OF TABLES

1.0 Introduction

The Navy, since the early 1950's, has been interested in the application of vertical and short take-off and landing aircraft for sea control missions. This concept has received increased attention during the last decade in an effort to reduce the size requirements of future carriers, provide a greater number of small ships the capability of launching and recovering aircraft and, as a result, allowing a greater dispersal of aircraft among the available ships.

One propulsion concept that has been pursued by the Navy for these applications is the thrust augmenting ejector and is schematically illustrated in Figure 1.1. The basic concepts behind this device are quite simple. The primary mass flow $\dot{m}_p$ is injected into a shroud or duct. This primary flow entrains and mixes with the secondary air within the duct. Because of the entrainment and mixing, the secondary air increases in velocity and the static pressure within the duct drops. This reduced pressure causes more ambient secondary air to be entrained at the inlet. As the mixed flow continues to move through the ejector the reduced static pressure is usually returned to ambient by passing it through a diffuser. The greater the effective area ratio A_3/A_2 that the diffuser is able to sustain, without separation, the lower will be the static pressure within the mixer and as a result the greater the inflow of secondary air. The advantage of such a device lies in the ability of the moving secondary stream to effectively interact with the primary flow and increase the energy exchange between the primary and secondary. This results in an increase in the exit momentum of the flow and causes the original thrust available from the primary nozzle to be amplified by some factor.

This amplification factor has been called the augmentation ratio (ϕ). Although there are several variants on the definition of augmentation ratio, the definition to be used throughout this report will be the total measured thrust or exit momentum minus the ram drag (if there is a free-stream velocity into the inlet) of the ejector system divided by the thrust that would be produced by all the primary and boundary-layer control nozzles due to an isentropic expansion of the same mass flow to ambient conditions. This definition normalizes the thrust of the ejector system to the maximum or ideal thrust that could be obtained from the same primary mass flow exhausting to ambient.

The augmentation or amplification of thrust that can be obtained with any given ejector system is a function of its geometric parameters, entrainment and/or mixing characteristics and the flow losses throughout the ejector. An example of the peak augmentation ratios that have been achieved by various experimentors is shown in Figure 1.2. Direct comparisons of ejector systems are difficult to make because of the wide differences in configuration and design. For this reason, the ejector designs listed in Figure 1.2 are characterized by means of several parameters. The main point to be seen from this figure is that isentropic

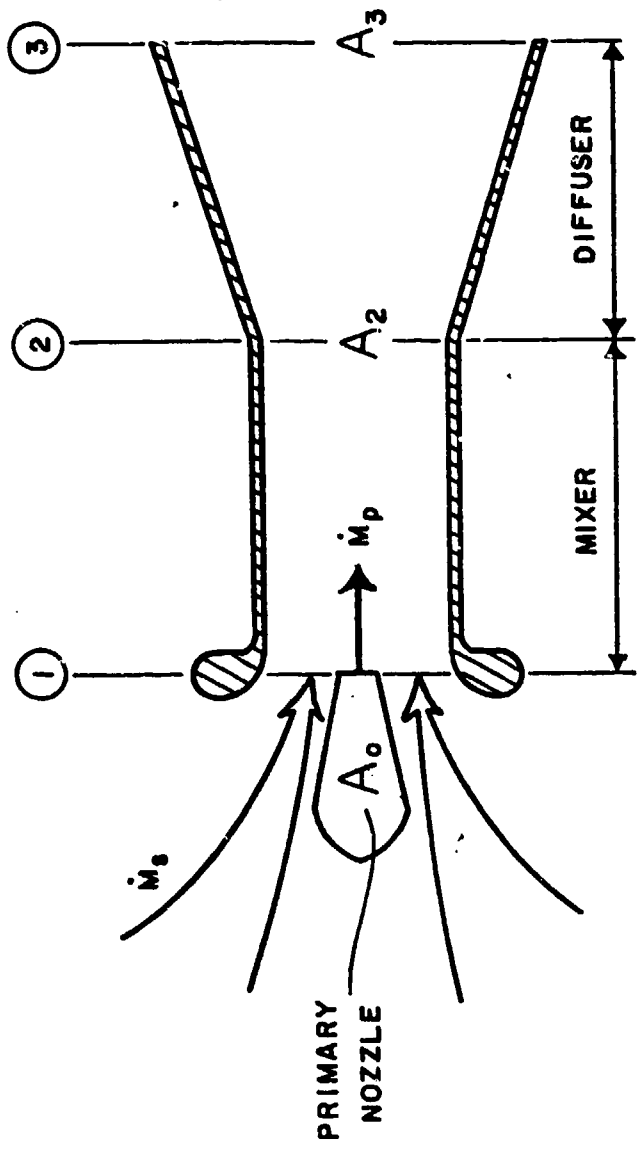

Figure 1.1 Schematic Illustration of Thrust Augmenting Ejector. $(A_1 = A_2 - A_0)$

EJECTOR CONFIGURATION	THROAT WIDTH	MIXER LENGTH	DIFFUSER LENGTH	SPAN	NPR	NTR	ϕ_{MAX}
Rockwell Cross-Slot Centerbody with Coanda Jets (Ref a)	4.88" (0.1239m)	———	7" (0.1778m)	20" (0.508m)	1.5-2.5	1.0	1.62
Aerospace Research Laboratories (ARL) Configuration "F" (Ref b)	10" (0.254m)	5" (0.127m)	45" (1.143m)	60" (1.524m)	1.01-1.27	1.0	2.00
Antiseparation Tailored Contour Ejector (Ref c)	10" (0.254m)	5" (0.127m)	11.75" (0.2985m)	60" (1.524m)	1.06-1.25	1.0	1.88
"STAMP" Jet-Diffuser Ejector (Ref d)	4" (0.1016m)	———	4.04" (0.1026m)	15"	1.25	1.05	2.09

Figure 1.2 Characteristics of Several High Performance Ejectors

thrust augmentation ratios from 1.6 to greater than 2.0 have been achieved in the laboratory. All of the examples shown in Figure 1.2 are steady flow ejectors, i.e., the flow from the primary nozzles is steady. There are classes of ejectors, however, for which the primary flow is unsteady or cryptosteady (i.e., it can be viewed as steady or unsteady depending upon the frame of reference of the observer). Although laboratory testing has shown that significant increases in entrainment at low pressure ratios have been obtained with such unsteady flows, their practicality for application, however, remains to be determined. For this reason, this report will only consider steady flow ejector systems.

Since it is desired to amplify the primary thrust as much as possible, i.e., obtain the maximum augmentation ratio, a great deal of effort is spent in designing primary and boundary layer control nozzles to effectively do this job. In most cases the necessary and detailed design requirements for these nozzles is very much dependent on the over-all configuration of the augmenter. By reducing the complex configurations to a much simplified format, that can be described in terms of a limited number of geometric parameters, and estimating the mixing characteristics as well as the typical flow losses that have been measured on ejector systems, it is possible to develop a first order estimate of performance. The sensitivity of the ejector to various loss mechanisms can be examined as well as gross parameters such as mass flow rates, velocities, thrust and augmentation.

In this study, four computer codes were available. The first was written at the NAVAIRDEVCEN and is based on the one-dimensional incompressible flow analysis outlined by Quinn, Viets and others (references (b), (e), and (f)). A second more complex one-dimensional analysis, because of its use of compressible flow relationships, was developed and reported by Salter (reference (g)). Dr. Salter provided a detailed listing of his computer code for use by the NAVAIRDEVCEN and it is upon this analysis that most of the computations shown in this report are based. This code was modified at the NAVAIRDEVCEN to allow for skewness at the diffuser exit and the incorporation of a jet-diffuser configuration. The third code was made available by the North American Aircraft Division (Columbus) of the Rockwell International Corporation. This is a two-dimensional finite difference analysis and is an extension on the original work of Gilbert and Hill (reference (h)). Both of the previous two computer codes are proprietary to Bell Aerospace Textron and Rockwell International Corporation respectively and are not generally available to industry. The fourth computer code, by far the most complex, is a three-dimensional finite element ejector analysis. This code is a variant within a much larger flow field analysis code and was developed at Bell Aerospace Textron under the sponsorship of NASA, Lewis, (reference (i)). Because of the complexity of this code and its potential for application over a wide range of flow conditions, it was extremely difficult to use. Input data was difficult to develop and running times were long. Because of these disadvantages, only limited use was made of this code. In fact, it was only run on a case where there was a mixing of two streams, one being a primary flow and the other a secondary or co-flowing field. To include the effects of multiple nozzles, a mixing section,

as well as a diffuser within the code would result in excessive running times. Even a solution for the mixing of two streams with a total of 28 nodal points ran for 30 seconds on the NAVAIRDEVCEN CDC 6600 computer. For the above reasons, this code was pursued no further and plans for additional ejector analyses were dropped.

The ejector code provided by Rockwell also has its limitations. It was designed specifically to analyze configurations that included both a centerbody primary flow and Coanda wall jets. It was not possible, without extensive alteration of the code, to eliminate the Coanda flows. Although the Rockwell code includes nozzle losses, turning efficiency for the Coanda flows, friction losses throughout the ejector and mixing losses, it does not include secondary inlet losses nor diffuser efficiency. In any case, the Rockwell code was only applied to specialized configurations with Coanda wall jets.

It must be noted that all of the codes examined in this report are basically built on the original analysis developed by von Karman (reference (j)), with increasing degrees of sophistication. A new approach to analyzing ejector flows has been introduced by Bevilaqua (reference (k)) and considers the ejector shroud as flying through a flow field of entrained air. In this technique the entrainment of the secondary air by the primary flow is developed from a viscid analysis. Once this entrained flow has been characterized it is replaced with line of sinks and the overall flow in and around the ejector is solved from an inviscid or potential approach using a vortex lattice. This method offers several distinct advantages in that the effects of adjacent bodies on the ejector flow can be included and details of the ejector shroud (being treated as a wing) can be examined. The impact of changes to the configuration of the inlet lips and/or diffuser flaps can be readily seen. Although this is a novel and interesting approach to ejector analysis it is still under development and will not be pursued in this report. Some simplified aspects of this approach, however, have been incorporated in the Rockwell version of the Gilbert and Hill code that was supplied to the NAVAIRDEVCEN

Although the simplified one-dimensional techniques and codes available will not provide detailed analysis for a complete internal design they should be most effective in the conceptual design stages in setting upper limits on augmentation as well as providing a more realistic limit when losses are included.

The following sections of this report will start with a simplified ideal (no loss) ejector configuration (see Figure 1.1). The sensitivity of gross parameters for the ejector will be examined with respect to variations in geometry and thermodynamic parameters. Flow losses will then be included and the sensitivity of the overall performance of the ejector system will be examined as a function of these losses. Having done this, several specific ejector systems for which experimental data is available will then be examined to determine the usefulness of these analyses, particularly the one-dimensional codes, for conceptual design studies.

2.0 Discussion of Results

2.1 General Characteristics: No Losses

Prior to introducing various flow losses within the ejector, it is of some interest to examine the response of an ideal ejector to various geometric and thermodynamic variations. In this case the simplified ejector configuration shown in Figure 1.1 will be used. This baseline ejector will have the following characteristics:

A_1/A_o =	20	T_a =	519°R (411.2°K)
A_3/A_2 =	1.8	P_a =	2116 LBF/FT^2 (1.013X10^5 Pa)
P_o/Pa =	1.3	W =	10" (0.25 m)
T_o =	519°R (411.2°K)	L_m =	5" (0.127m)
V_a =	0.0 m/sec	L_d =	23" (0.584 m)

From this baseline, the following variants have been examined:

10.0	$\leq$	A_1/A_o	$\leq$	30
1.0	$\leq$	A_3/A_2	$\leq$	2.2
1.3	$\leq$	NPR	$\leq$	2.3
520°R	$\leq$	T_o	$\leq$	1460°R
520°R	$\leq$	T_a	$\leq$	620°R
0.0	$\leq$	V_a	$\leq$	100 ft/sec (30.48 m/sec)

2.1.1 Geometry

The one-dimensional compressible analysis will be primarily used for these variations. It is of interest, however, to compare the computations for augmentation ratio using the one-dimensional compressible and incompressible codes. This comparison is shown in Figure 2.1 A&B. It is clear that some deviation, although slight, does exist. This deviation is most pronounced at high values of A_3/A_2 and low values of A_1/A_o. In both of these cases the secondary velocity is high and compressibility effects are to be expected. Because of its greater flexibility and ability to handle thermodynamic variations the one-dimensional compressible code will be used to examine the additional variations.

In Figure 2.2 A&B the effects on the secondary to primary velocity ratio ($\bar{V}_S/\bar{V}_P$), mass flow ratio ($\dot{M}_s/\dot{M}_P$) and efficiency of energy transfer are illustrated as functions of inlet and diffuser area ratio. The transfer efficiency in this case is defined as the ratio of the kinetic energy of the ejector efflux to the kinetic energy of the primary stream. The mass flow ratio increases with both A_3/A_2 and A_1/A_0. The velocity ratio, however, increases with A_3/A_2 but decreases with A_1/A_0. The efficiency of energy transfer, it will be noted, follows the trend of the velocity ratio $\bar{V}_S/\bar{V}_P$. That is, a decrease in the velocity ratio will cause a decrease in the efficiency of energy transfer. This does not necessarily imply that the augmentation ratio will be decreasing (as can be seen in Figure 2.3) but rather that the efficiency with which thrust is being amplified is decreasing. For example, when one examines the baseline configuration, it can be shown that:

$$\left.\frac{\Delta \phi}{\Delta(A_3/A_2)}\right|_{A_1/A_0=20} \gg \left.\frac{\Delta \phi}{\Delta(A_1/A_0)}\right|_{A_3/A_2=1.8}$$

Hence, it would appear that greater leverage on augmentation ratio is achieved by increasing the diffuser area ratio (assuming no separation) than by increasing the inlet area ratio.

2.1.2 Primary Temperature

An example of the importance of the secondary to primary velocity ratio can be seen when the primary stagnation temperature is increased. Figure 2.4 illustrates dramatically that although the isentropic nozzle thrust is remaining relatively constant, the total ejector thrust and augmentation ratio are decreasing. It will be noted that the velocity ratio and efficiency of energy transfer are also decreasing while, at the same time, the mass flow ratio is increasing. Although increased entrainment and secondary mass flow are important, one must be careful when looking at an increased mass flow ratio not to infer an increase in augmentation ratio. The secondary to primary velocity ratio appears to be a better indicator in this regard.

2.1.3 Secondary Temperature

If one takes the opposite point of view, and the ambient or secondary air temperature is increased, it can be seen from Figure 2.5 that $\bar{V}_S/\bar{V}_P$ increases slightly and $\dot{M}_S/\dot{M}_P$ decreases slightly over the temperature range examined (520°R to 620°R). Again, both total ejector thrust and augmentation ratio increase slightly. This point is of interest for two reasons. First, it again illustrates the importance of the secondary to primary velocity ratio. Secondly, it would indicate that augmenters should not be sensitive to reingestion of the warm exhaust gases back into the secondary flow. In fact, a slight improvement might be anticipated. This, of course, is in strong contrast to the degradation of primary power plant thrust with increasing ambient or inlet temperature.

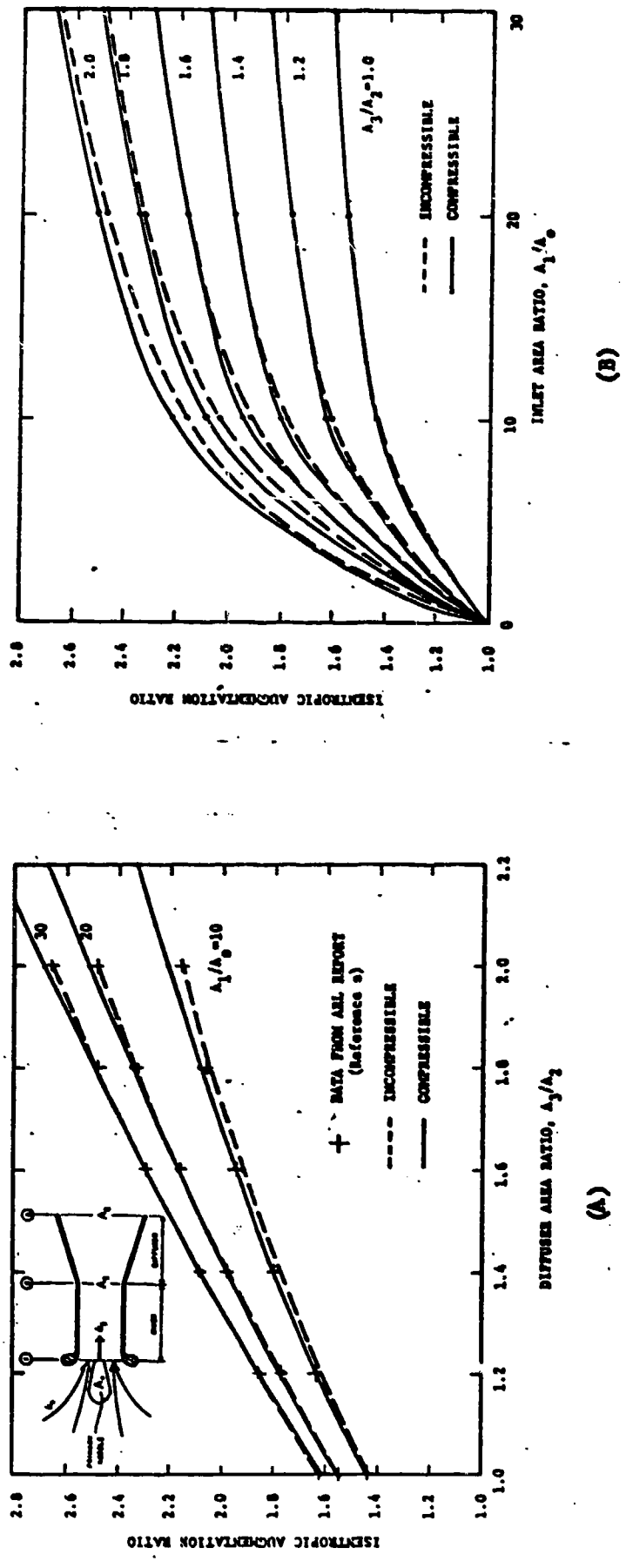

Figure 2.1 Ideal Augmentation Ratio Characteristics as a Function of Inlet and Diffuser Area Ratios

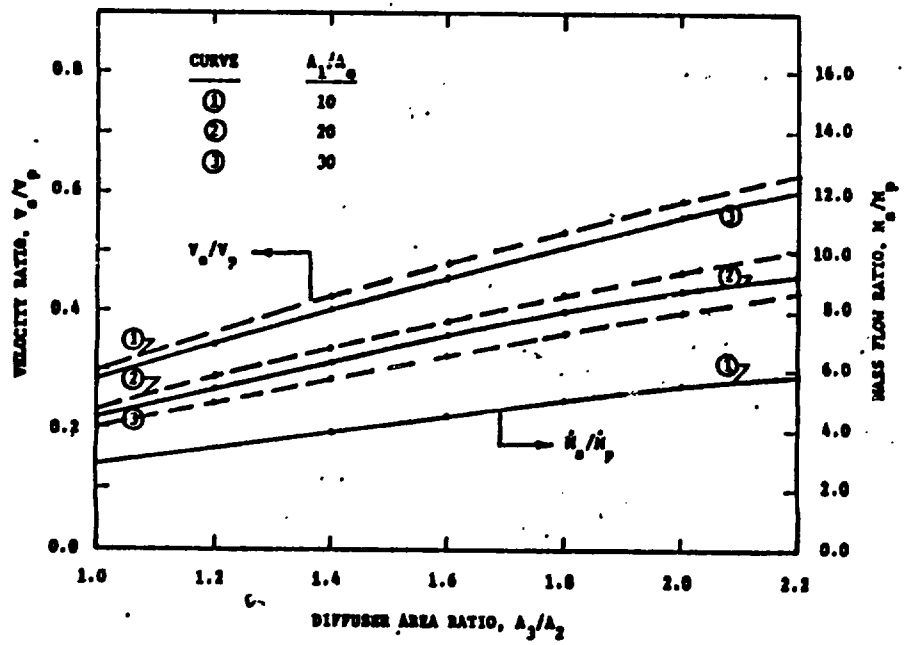

(A)

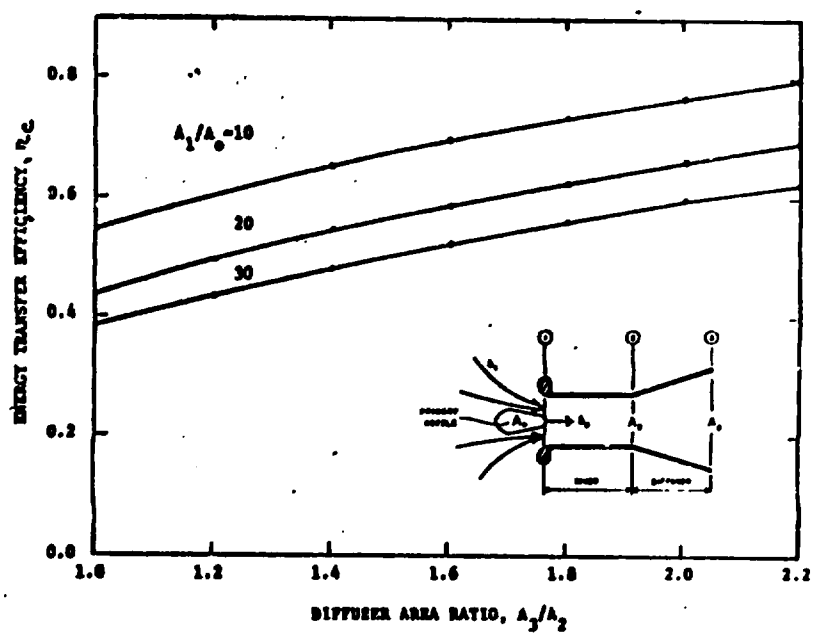

(B)

NADC-80094-60

Figure 2.2 Ideal Velocity Ratio, Mass Flow Ratio and Energy Transfer Efficiency as a Function of Diffuser Area Ratio.

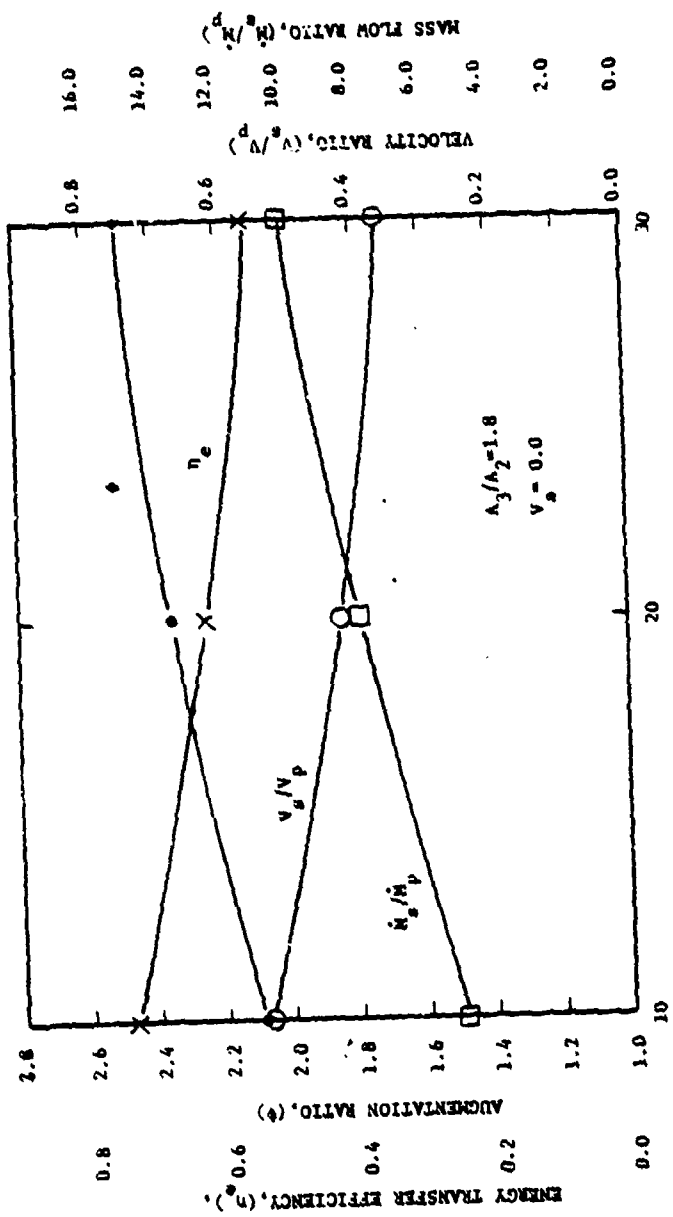

Figure 2.3 Ideal Ejector Characteristics as a Function of Inlet Area Ratio.

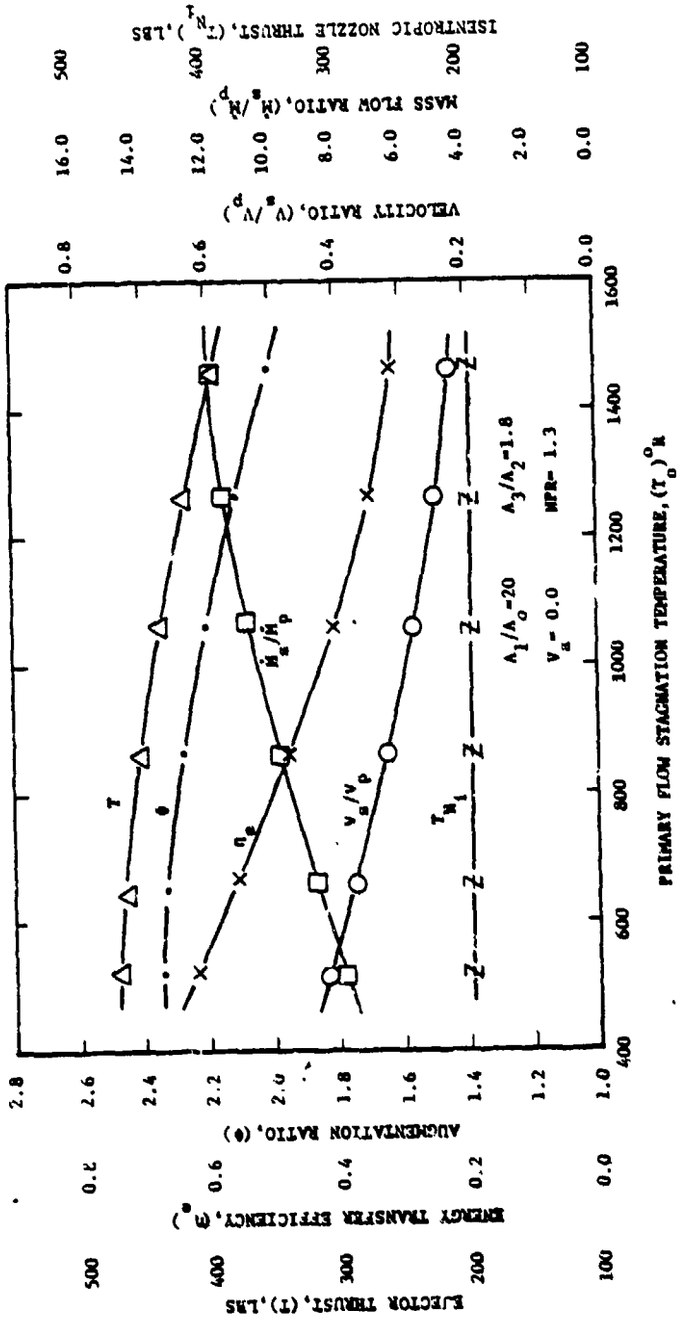

Figure 2.4 Ideal Ejector Characteristics as a Function of Primary Flow Stagnation Temperature.

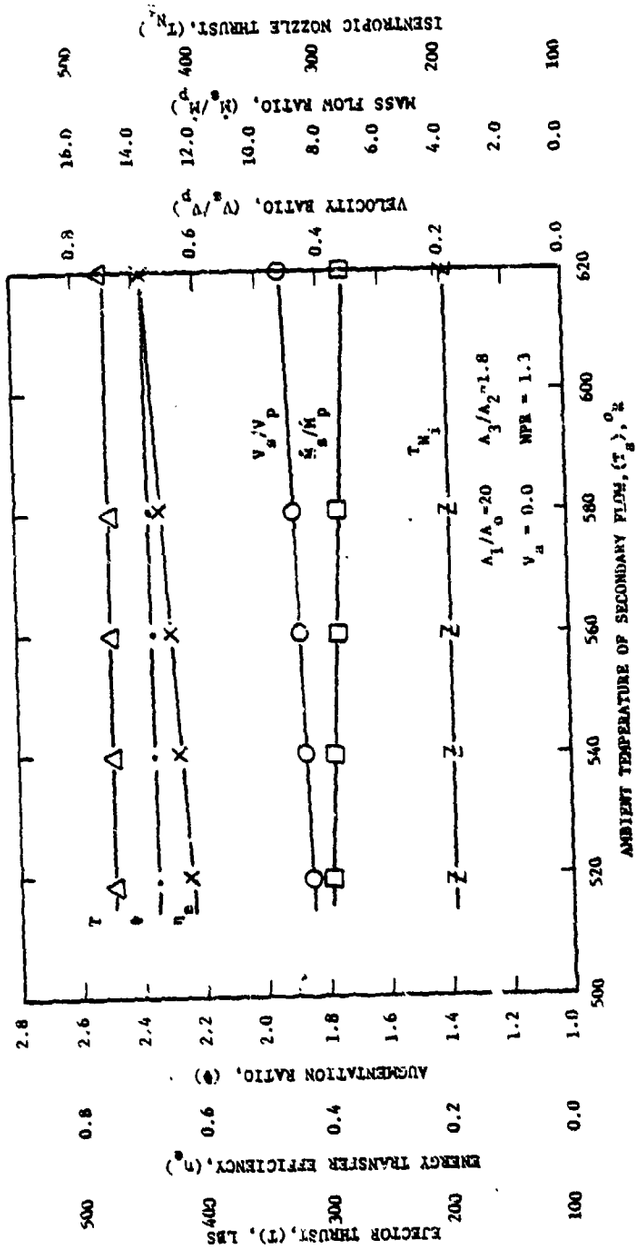

Figure 2.5 Ideal Ejector Characteristics as a Function of Ambient Temperature of Secondary Flow.

2.1.4 Nozzle Pressure Ratio

The effects of variations of primary nozzle pressure ratio on the baseline ejector is shown in Figure 2.6. Here it can be seen that both the isentropic nozzle thrust and the total ejector thrust increase significantly. Augmentation ratio, however, increases only slightly. It is interesting to note that the secondary to primary velocity ratio increases significantly and is contrary to what one might expect intuitively. This effect is due to the primary nozzle being choked and as a result, assuming a convergent nozzle, the primary exit velocity is fixed at the sonic condition. It will be noted in Figure 2.6, however, that the mass flow ratio is decreasing and again is out of phase with the augmentation ratio.

2.1.5 Free Stream Velocity

If the ejector is mounted in such a way that the secondary inlet is perpendicular to an ambient free stream velocity, the gross augmentation ratio will increase substantially. The net augmentation ratio (and the actual thrust), however, will decrease due to the ram drag induced. Figure 2.7 illustrates these effects for the baseline ejector. It will be noted that secondary to primary velocity and mass flow ratios increase as does the efficiency of energy transfer. The net or useable augmentation ratio, however, decreases rapidly.

To make use of an ejector in forward flight, therefore, one would want to minimize the ram drag, i.e., $\dot{M}_s \bar{V}_a$. Since $\bar{V}_a$ is a fixed quanitity, the only variable available for reduction is the secondary mass flow. It would appear, therefore, that the goal would be to decrease $\dot{M}_s/\dot{M}_p$, increase $\bar{V}_s/\bar{V}_p$ and concurrently increase the augmentation ratio. This theoretically could be accomplished by reducing T_o/T_a and increasing P_o/P_a. This comparison is made in Figure 2.8 where the baseline configuration, with a free stream velocity of 150 ft/sec (45.7 m/sec) is examined with increasing values of T_a and nozzle pressure ratio. It can be seen in this situation that both the ejector net thrust and the net augmentation ratio are now increasing. It will also be noted, compared to Figure 2.7, that the velocity ratio is substantially increasing but the corresponding mass flow ratio is now decreasing. The large increase in the velocity ratio ($\bar{V}_s/\bar{V}_p$) is again due to the fact that the primary nozzle is choked and, therefore, $\bar{V}_p$ remains fixed at the sonic condition. In any case, it may be possible to overcome some of the deleterious effects of ram drag on an ejector moving at a forward speed perpendicular to the inlet by carefully controlling the thermodynamic conditions. Alperin (reference 1) has also examined these possibilities analytically and has included variations in the ejector geometry to minimize the ram drag losses and develop useful ejector thrust for both subsonic and supersonic applications.

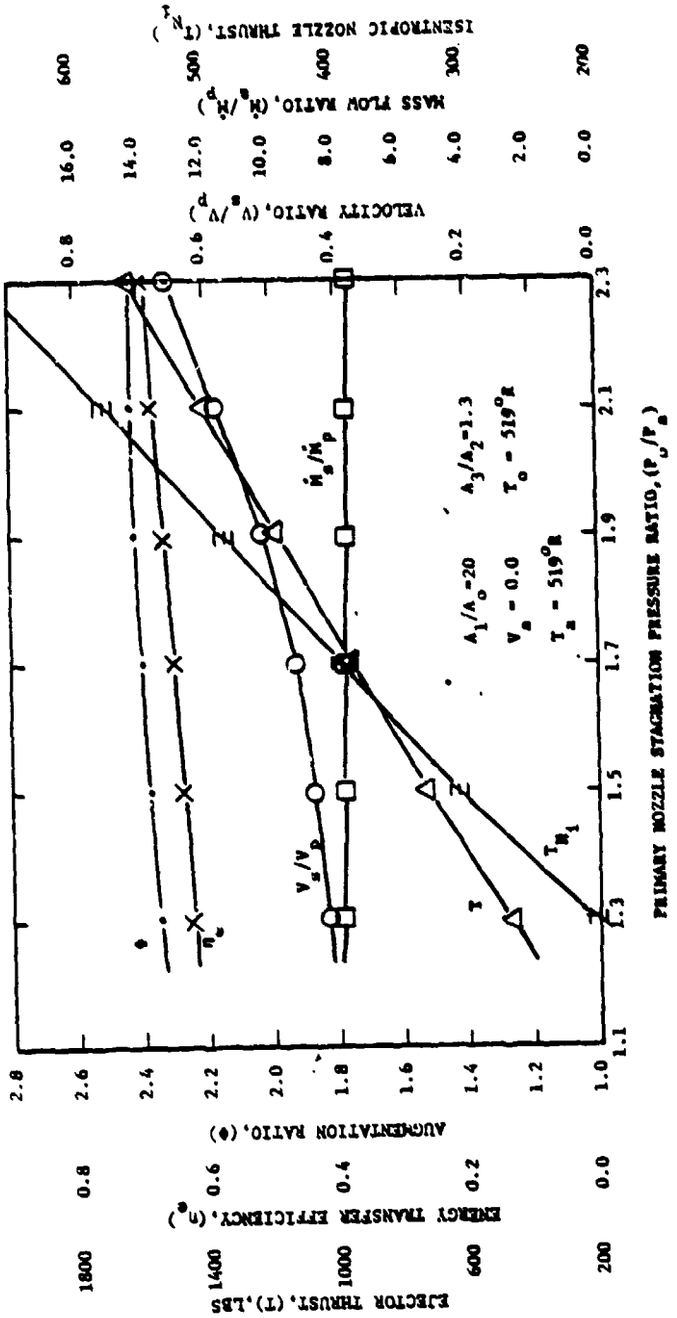

Figure 2.6 Ideal Ejector Characteristics as a Function of Primary Nozzle Stagnation Pressure.

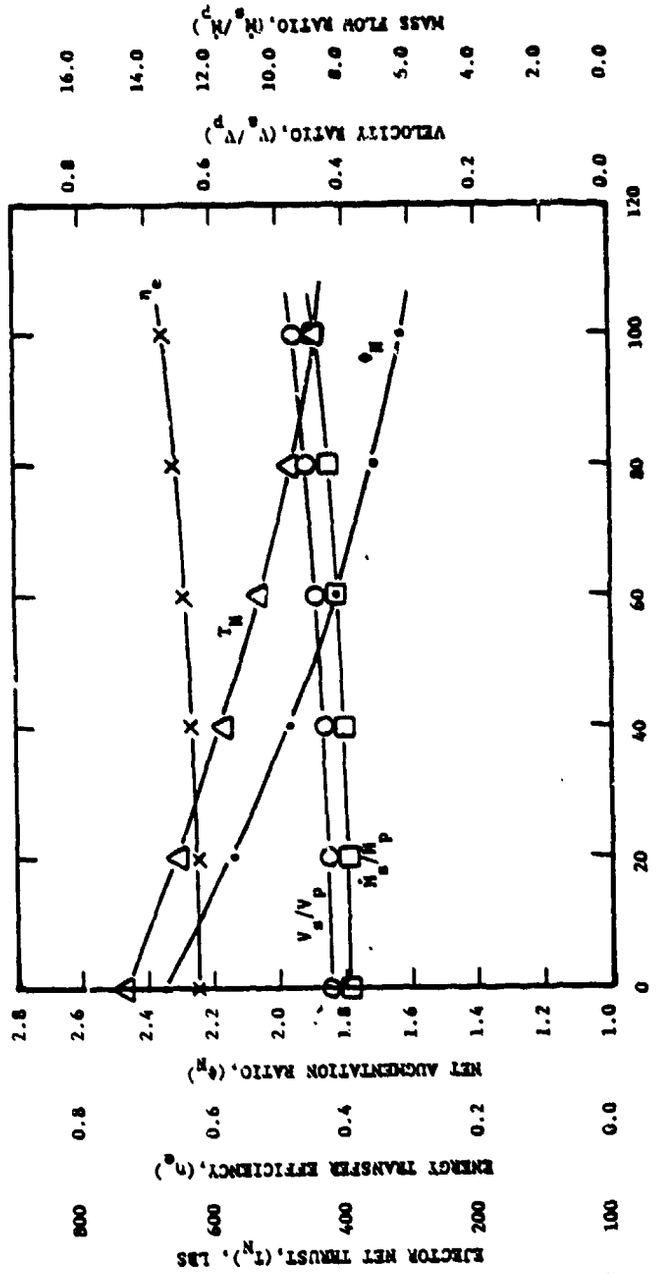

Figure 2.7 Ideal Ejector Characteristics as a Function of Free Stream Velocity.

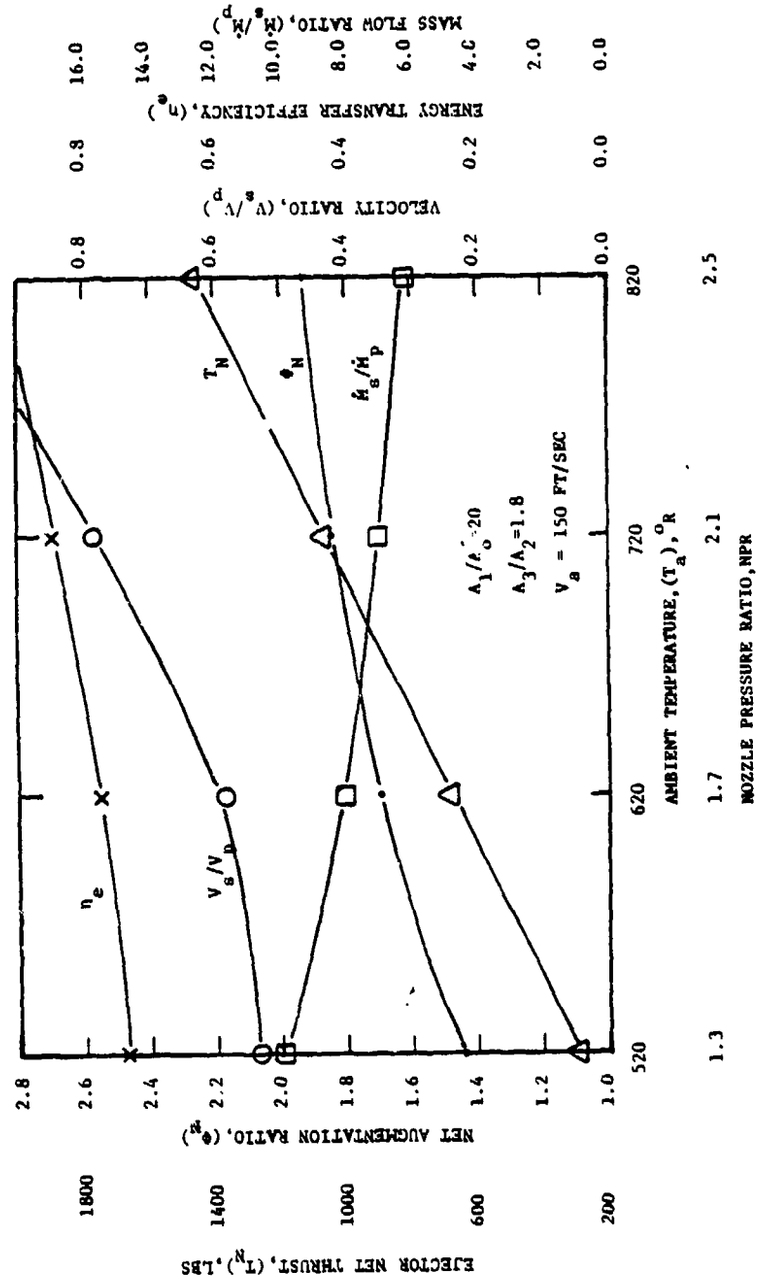

Figure 2.8 Decreasing Ram Drag Effect by Increasing P_o/P_a and Decreasing T_o/T_a for a Constant Free Stream Velocity.

2.2 Losses

Up to this point, no internal flow losses have been considered and these losses can have a significant impact on the overall performance of the ejector. Certainly for a conceptual design estimate, a realistic augmentation ratio, total ejector thrust, as well as secondary and primary mass flows and velocities are quantities that are needed because of their impact on power plant requirements and overall aerodynamic design. In order to arrive at a more realistic estimate of these values, five types of loss mechanisms have been considered for the simplified ejector configuration shown in Figure 1.1. These are:

Inlet losses

Primary nozzle efficiencies

Friction losses in the mixing section

Mixing effectiveness

Diffuser efficiencies

All of these loss mechanisms have been incorporated in both the one-dimensional incompressible and compressible codes. This is not necessarily true for the more complex two and three dimensional mixing codes. In most cases these codes only consider the friction losses and mixing effectiveness.

All of the above losses are treated as empirical parameters that can be estimated by means of well developed relationships (for example, the friction losses), from recent experimental data on similar ejector systems, or experience. Even the most sophisticated mixing codes incorporate a variety of constants in the turbulence models that have been "tuned" with experimental data until reasonable agreement was found. Application of these mixing codes to ejector analysis often requires estimates of inlet conditions until agreement is found with experimental exit conditions. Once this has been accomplished parametric variations around the norm can be accomplished.

The purpose of this section is to illustrate the form of these various loss mechanisms as used in the one-dimensional codes, indicate nominal values for these parameters that have been measured experimentally and demonstrate their sensitivity to overall ejector performance.

secondary or entrained

(1)

nts for the additional
imary nozzles by the secondary
can be written:

$- C_D A_s/A_1$) (2)

coefficient based on a
meters K_1 and $C_D \frac{A_s}{A_1}$

(3)

for inlet losses, primarily
, are in terms of ξ_1, this
itivity of the ejector to

ll be expressed as:

(4)

(5)

ction due to wall friction

(6)

otation:

(7)

where A_{ref} is the wetted perimeter of the mixing section, C_f is the skin friction coefficient for a flat plate and $\bar{V}_{ref}$ is a reference velocity that would normally be taken as the average velocity at station 2, that is, the end of the mixing section. β_2 will be discussed in Section 2.2.4. The skin friction coefficient for a flat plate with a turbulent boundary layer can be expressed empirically as:

$$C_f = 0.074(\bar{V}_{ref} \cdot L_m/\upsilon)^{-0.2} \tag{8}$$

In the case of an ejector configuration that injects the primary fluid along the wall or uses high velocity wall jet boundary layer control, $\bar{V}_{ref}$ may be substantially higher than $\bar{V}_2$ and as a result the value of ξ_f could increase substantially. In terms of a friction factor, f, related to pipe flow, ξ_f can be written:

$$\xi_f = fL_m/2D_h\beta_2 \tag{9}$$

Where $f = 4\,(\bar{V}_{ref}/\bar{V}_2)^2 C_f$, L_m is the length of the mixing section, and D_h is the hydraulic diameter.

$$D_h = 2A_2/(h+w) \tag{10}$$

As a result, the pressure drop due to friction in the mixing section (equation (6)) can be rewritten in the format used by Salter as:

$$\Delta P_f = (f\, L_m / 2D_h)\, \rho_2\, \bar{V}_2^2 \tag{11}$$

2.2.4 Mixing effectiveness

Mixing effectiveness within the one-dimensional ejector codes is handled by introducing a flow skewness parameter. This parameter is provided as input to these simplified codes and determines how far the velocity profile deviates from an ideal fully mixed condition, i.e., a uniform velocity profile. The skewness parameter (β_i) is defined as the momentum flux through a given area A_i divided by the momentum flux due to a uniform mass average velocity profile. That is:

$$\beta_i = \int_{A_i} \rho\, v_i^2\, dA \;/\; \rho\, \bar{V}_i^2\, A_i \tag{12}$$

If the flow is completely mixed and the velocity is uniform, $\beta_i = 1.0$. The values of β_i increase above unity as the flow becomes more non-uniform. One can express the actual momentum flux through a given area in terms of a momentum flux due to a uniform mass average velocity profile times its appropriate skewness parameter. It will be assumed, in what follows, that the velocity profile of both the primary flow and secondary flow entering the mixing section inlet are uniform. The skewness of each of these flows, therefore, will be assumed to be unity. Their individual velocities, however, would be significantly different. Skewness at the end of the mixing section (or start of the diffuser) and at the exit of the diffuser will be allowed to assume non-unity values. As will be shown later, these skewness values will have a significant impact on the overall performance of the ejector.

The ejector analyses that are used in the simplified one-dimensional codes consider the energy and momentum exchange process to occur in the defined mixing section. For this reason a skewness value (estimate of the extent of mixing) must be specified at the end of this mixing section. Measured values of skewness, however, are usually made at the exit of the diffuser. It cannot be assumed that these measured values at the exit of the diffuser are the same as at the start of the diffuser (i.e., the end of the mixing section). In fact, there is a considerable body of experimental evidence (references n, o, and p) indicating that the skewness may increase or decrease as the flow passes through the diffuser depending upon the direction of diffusion with respect to the skewed velocity profile. Diffusion in the plane of the velocity profile reduces mixing and increases skewness. Diffusion out of the plane of the velocity profile, i.e., perpendicular to the velocity profile enhances mixing and reduces skewness. Although the one-dimensional relationships developed by Quinn include the skewness terms both at the end of the mixing and diffusion sections, a relationship between the two is not provided. The code developed by Salter, on the other hand, only includes the skewness at the end of the mixing section and assumes the value for skewness at the exit of the diffuser to be unity. Although this may be approximately true for the special cases he examined, it would not be true in general. In most cases, experimental data on skewness would only be available at the exit of the diffuser. For this reason the expression for (ϕ) in the Salter code was modified such that a skewness value at the exit of the diffuser appears. That is:

$$\phi = \frac{\int_{A_1} \rho_3 v_3^2 \, dA}{V_N' \int_{A_o} \rho v_o \, dA} = \frac{\beta_3 \dot{m}_3 V_3}{V_N' \dot{m}_o} \qquad (13)$$

Equation (13) would suggest that the augmentation ratio can be increased by increasing β_3. The skewness at the end of the mixing section (β_2), however, is related to β_3 and increasing β_3, for a given diffuser area ratio, will impact the value of β_2. As will be seen later, the value of β_2 is a driving parameter in the ejector operation and in general an increase in β_2 results in reduced ejector performance.

Based on the limited data available from references f, n, o, and g, a relationship between β_2 and β_3 has been developed. This relationship, as mentioned previously, will depend on whether the diffusion process is occurring in or out of the plane of the velocity profile. The following relationships have been postulated:

Diffusion in the velocity profile plane,

$$\beta_3 = \beta_2^{(A_3/A_2)^2} \qquad (14)$$

Diffusion perpendicular to the velocity plane,

$$\beta_3 = \beta_2^{(A_2/A_3)^2} \tag{15}$$

Hence skewness increases for diffusion in the plane of the velocity profile and decreases for diffusion out of the plane (or perpendicular) to the plane of the velocity profile. These expressions provide reasonable agreement with available skewness data and, as will be shown later, allow for reasonable estimates of augmenter performance to be made if skewness values of either β_2 or β_3 are known or can be approximated based on previous experience.

2.2.5 Diffuser efficiency

Losses within the diffuser can be expressed in terms of a diffuser pressure coefficient ($\overline{C}_p$) as does Quinn or in terms of a diffuser efficiency (η_D) as does Salter. These two terms are related as follows:

$$\overline{C}_p = (\eta_D C'_p)/\beta_2 \tag{16}$$

where $C'_p = 1 - (A_2/A_3)^2$ and is the ideal incompressible pressure coefficient.

Efficiencies for a well designed diffuser have the general characteristics shown in Figure 2.9. That is, they typically increase with diffuser half angle until the flow separates. The point or angle at which separation occurs in an ejector diffuser obviously is dependent upon the specific design and the amount of boundary layer control (BLC) within the diffuser. The configurations studied by Quinn at the Aerospace Research Laboratories, which had a minimum of BLC, typically separated at half angles from approximately 5° to 9°. The Rockwell International ejectors that make use of Coanda wall jets to enhance entrainment as well as provide boundary layer control in the diffuser, typically separate at approximately 16° half angle. The Alperin jet-diffuser concept, with its relatively high blowing rate for BLC as well as increasing its effective diffuser area ratio has gone to half angles as high as 60° without separation. Once diffuser stall or separation occurs, however, augmentation ratio falls off rather abruptly as will be seen in some of the experimental data in Section 2.3.

2.2.6 Ejector sensitivity to losses

Having listed the five loss mechanisms that are included in the one-dimensional codes, it is of interest to know how sensitive the overall augmenter performance is with respect to each of the losses. In order to show this sensitivity, a range of values have been selected for each loss parameter and the resultant change in augmentation ratio, normalized to the ideal augmentation ratio, caused by each parameter in turn, is displayed in Figure 2.10.

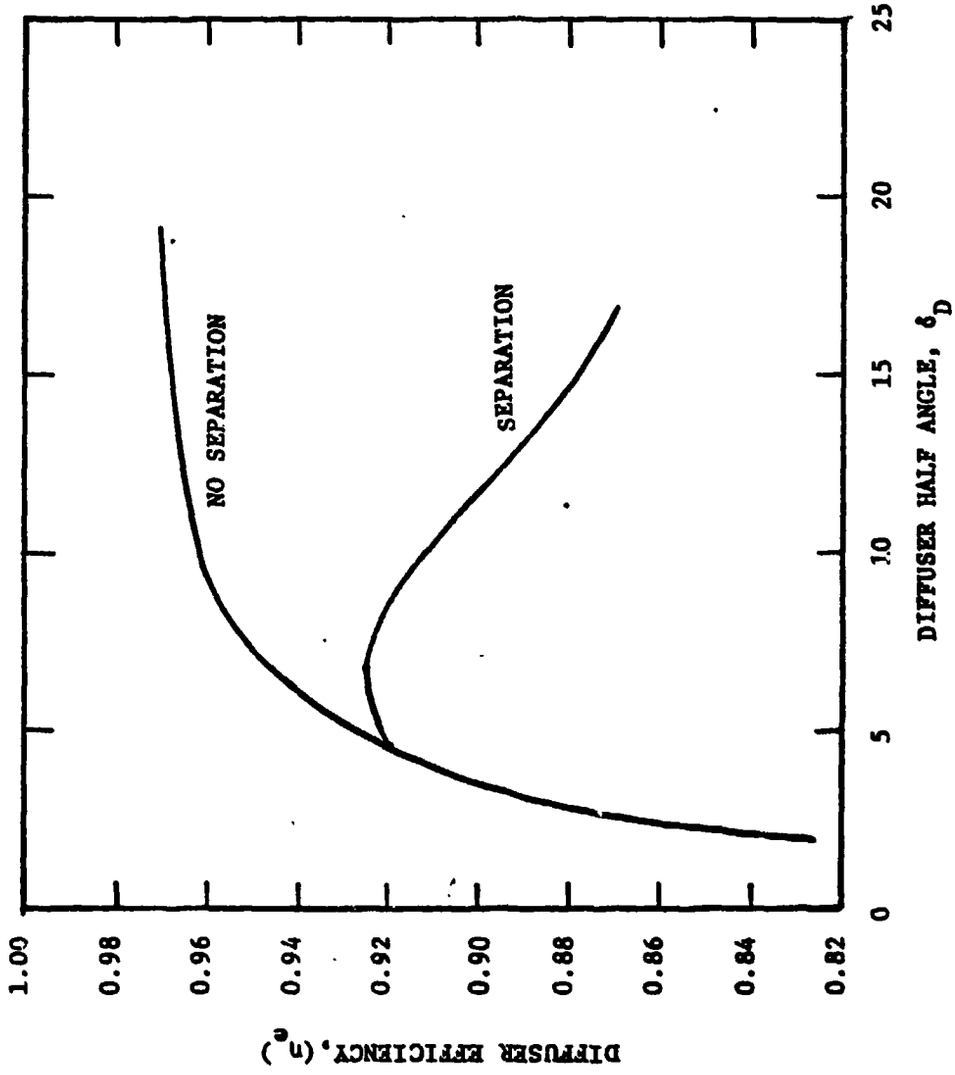

Figure 2.9 Characteristic Diffuser Efficiency

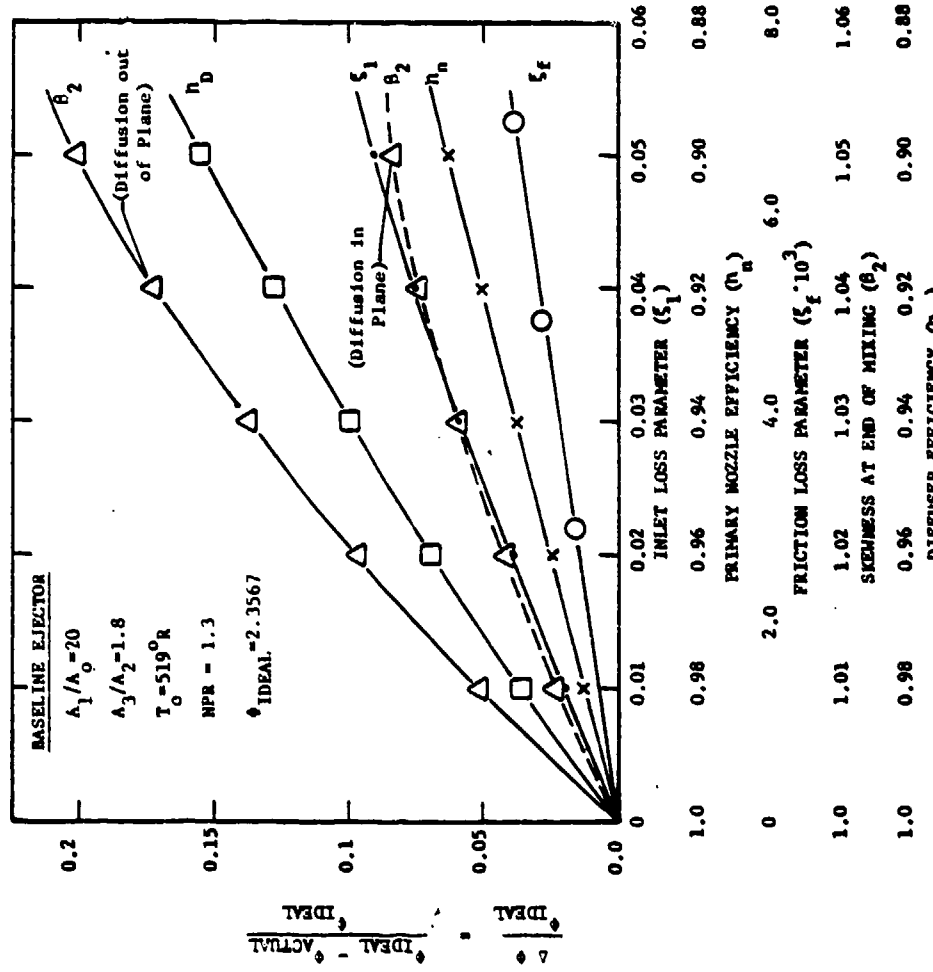

Figure 2.10 Sensitivity of Baseline Ejector to Loss Parameters

The baseline configuration previously discussed for the ideal case was used for this comparison and the range of values used for the loss parameters are as follows:

Inlet loss	$0.00 \leq \xi_1 \leq 0.050$
Primary nozzle efficiency	$0.88 \leq \eta_N \leq 1.00$
Friction losses	$0.00 \leq \xi_f \leq 0.007$
Diffuser entrance skewness	$1.00 \leq \beta_2 \leq 1.05$
Diffuser efficiency	$0.88 \leq \eta_D \leq 1.00$

This figure also illustrates the effects of diffusion in and out of the plane of the velocity profile.

The range of values chosen for each of these parameters was based on values that had been measured at ARL and/or some current work that is being done by the Rockwell International Corporation on the XFV-12A augmenter wing aircraft technology demonstrator. Over this range of parameters, it is clear that the skewness of the mixing section (β_2), provided the diffusion process is out of the velocity plane, is by far the most sensitive parameter in driving the augmenter performance. If the diffusion process is in the velocity plane or if the skewness is very low, the driving parameter then appears to be the diffuser efficiency. Care must be taken when examining these results, however, since only one parameter is allowed to vary at a time and all others are assumed to remain at these ideal values. In actuality, things are not totally independent and a diffusion process in the velocity plane which causes the skewness factor β_3 to increase and as a result increases the augmentation ratio, is neglecting the fact that the diffuser efficiency is a function of skewness and may be decreasing as β_3 is increasing. The net result would be that $\Delta\emptyset/\emptyset_{ideal}$ would be substaintially higher for the diffusion in the velocity plane case than illustrated in figure 2.10. Diffusion processes both in and out of the velocity profile plane were examined by ARL. The best known of the ARL ejector configurations was that used by Quinn where the diffusion was out of the plane of the velocity profile and therefore the skewness is decreasing as the flow passes through the diffuser.

The effective diffuser exit skewness for the Alperin Jet Diffuser Ejector has been estimated (based on experimental data taken at the Naval Air Propulsion Center) to be approximately 1.05. Since this diffusion process is in the plane of the velocity profile, the skewness at the throat or start of the diffuser can be estimated from equation (14) to be approximately 1.004. Since these values of skewness are so low, one might assume the diffuser efficiency is dominating the loss mechanisms. Estimating the diffuser efficiency, however, it would appear to be very high, assuming a diffuser half angle of 45° with no separation. The almost ideal values for both mixing skewness and diffuser efficiency probably account for this ejector's excellent performance.

Other augmenter configurations currently under investigation for application to the XFV-12A technology demonstrator have given measured skewness values from 1.05 to 1.15 at the diffuser exit. The diffusion process, in this case, is also in the plane of the velocity profile and, therefore, the skewness at the entrance to the diffuser is lower than at its exit. With these exit skewness values one might again suspect the diffuser efficiency to dominate the ejector losses.

Mixing section friction losses are consistently the least important to the augmenter performance. The loss parameter ξ_f is a function of the friction coefficient, reference velocity and mixing section length. It appears however, that unless these values are exceptionally large only a small degradation is seen in ejector performance.

Reasonable values for primary nozzle efficiencies and inlet loss parameters do not appear to drive the performance, although for low inlet area ratios and high diffuser area ratios (and consequently high secondary flow velocities) inlet losses can become substantial.

It is now of interest to apply these codes to the performance estimation of actual laboratory ejectors that have been built and tested and for which there are experimental data on the total ejector performance as well as some limited data on the loss parameters. It is clear from the foregoing that, if loss parameter data is not available, the skewness and diffuser efficiency are the most difficult to estimate because of their high sensitivity. Three basic configurations will be examined. The first are those configurations studied by Quinn at ARL. The second are basic configurations being used by Rockwell International and include a centerbody nozzle with Coanda wall jets on the diffuser shrouds. The third is the Alperin Jet-Diffuser ejector developed by the Flight Dynamics Research Corporation as part of the Navy's Small Tactical Air Mobility Platform (STAMP) Program.

2.3 Comparisons with Experimental Data

2.3.1 ARL Configurations

By far the best known experimental work with high augmentation ratio ejectors is that conducted by Quinn at the Aerospace Research Laboratories. Reference b discusses the experimental configurations studied and the results that were obtained. The main variations were in mixing section and diffuser length with the results shown in terms of augmentation ratio versus diffuser area ratio. What appears clear in these results (reproduced in Figure 2.11) is that the ejectors all exhibit the same characteristics and approximate augmentation up to a diffuser area ratio of approximately 1.5. At this point both configurations B and D show a sudden decrease in augmentation ratio indicating a diffuser stall. As can be seen from Table 1, diffuser stall sets in at diffuser half angles from 5-9 degrees and is based on the point of maximum diffuser efficiency (see Figure 2.12) or the point where the rise in augmentation just starts to degrade.

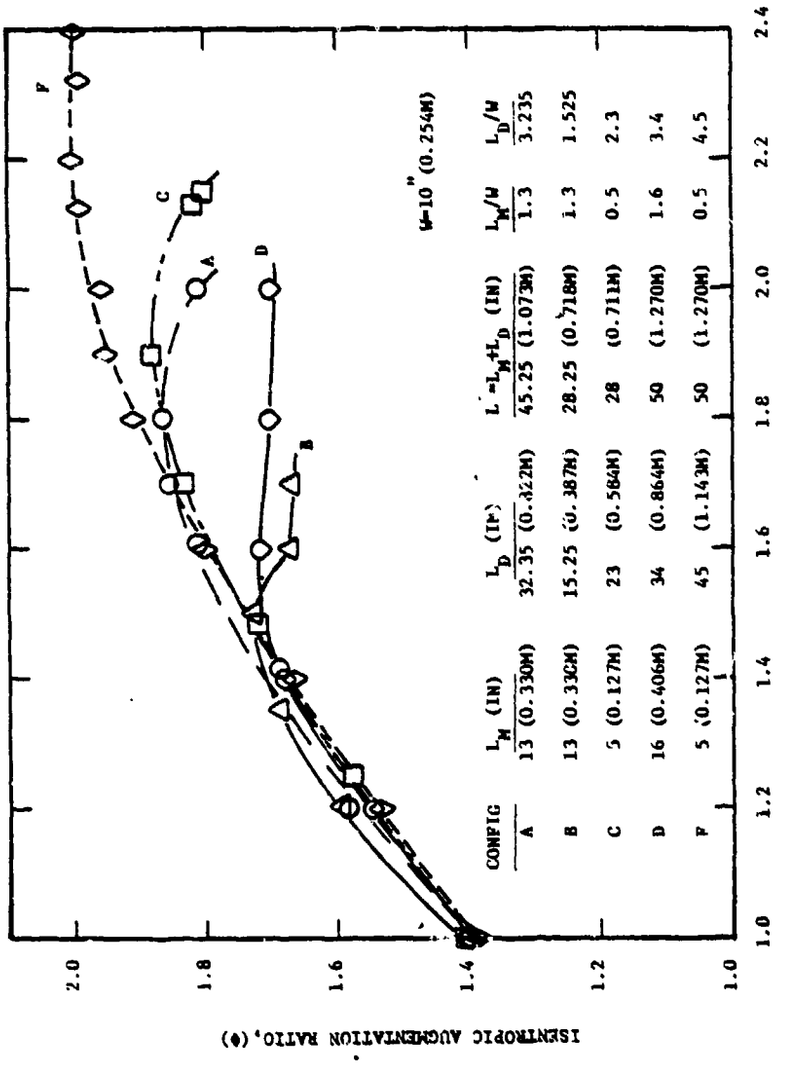

Figure 2.11 ARL Experimental Data Showing Effect of Mixing Section and Diffuser Length (Reference b)

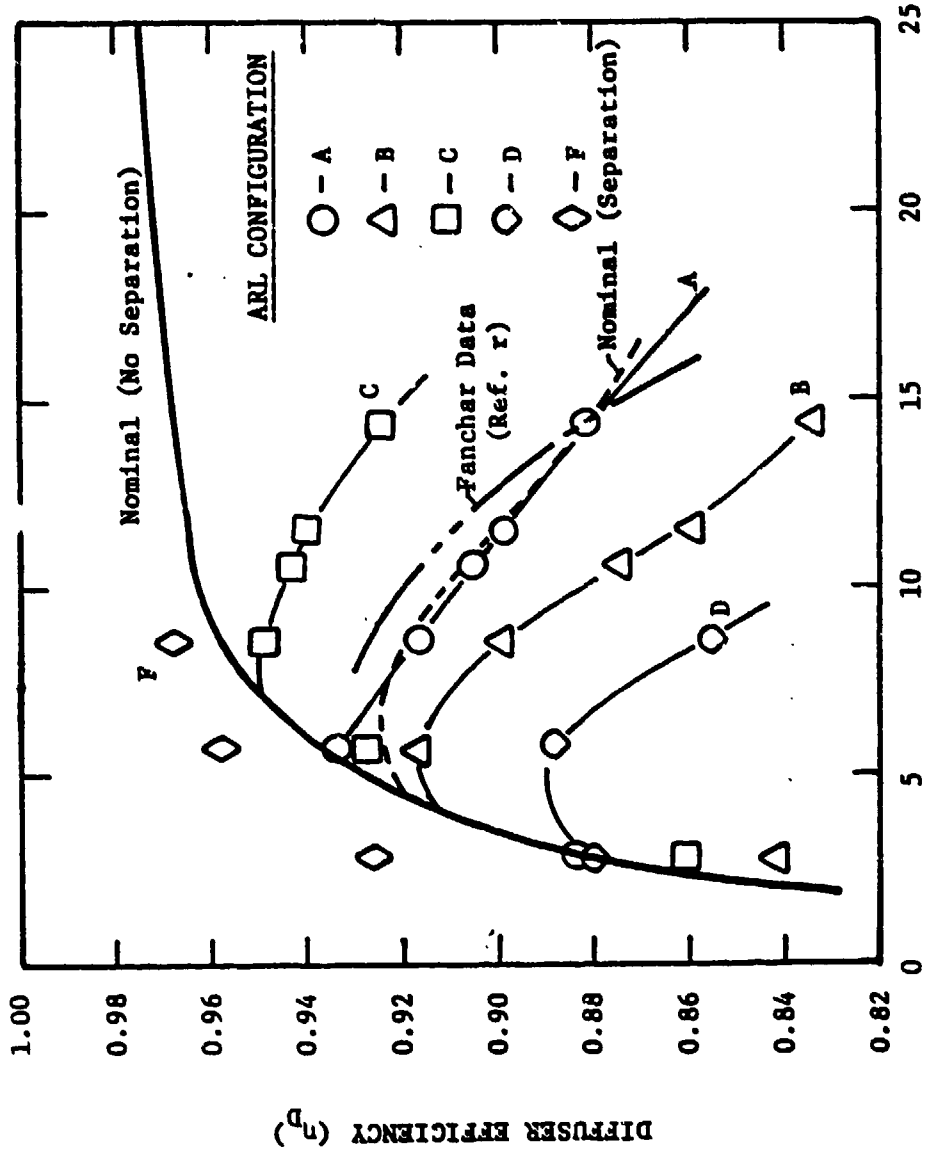

Figure 2.12 Diffuser Efficiencies for ARL Ejectors.

Table I
STALL CONDITIONS FOR ARL DIFFUSERS

Configuration	A_3/A_2	δ_D(deg)	η_D(max)
A	1.65	5.8	0.934
B	1.35	5.8	0.917
C	1.6	7.5	0.950
D	1.47	5	0.89
F	2.4	9	0.97

The design point for the ARL work was configuration A. Computations had been made to determine the length of the mixing section such that the spreading primary flows would just reach the mixer walls before entering the diffuser. This length had been determined to be 13 inches. Increasing the mixer length to 16 inches in configuration D causes the spreading primary flow to intercept the walls prematurely with a resultant increase in friction losses. It is doubtful, however, that friction losses alone should cause such a rapid degradation. Bevilaqua in reference g also noted this effect with increasing hypermixing angles on the primary nozzles, although the degradation in performance does not appear to be as severe as in the case of configuration D.

Making use of the one-dimensional codes, the performance characteristics (augmentation ratios) for the ARL configurations can be estimated. In order to make these computations, however, values for the various loss parameters must be assumed. Experimental work conducted at ARL has provided reasonable estimates for these parameters which are listed as follows:

Inlet loss parameter (ξ_1)----------0.025

Primary nozzle efficiency (η_N)----------0.96

Friction factor (f)----------0.0078-0.0211

Mixing effectiveness (β_2)----------1.01-1.04

Diffusion efficiency (η_D)----------0.83-0.96

The friction factor has been computed in this case by first assuming the ejector is ideal (i.e., no losses) and determining a value for $\bar{V}_2$. Now using this value in equation (8) as $\bar{V}_{ref}$, a value for the friction coefficient over a flat plate can be determined. This value along with $\bar{V}_2$ is then substituted into equation (7) to determine ξ_f. Equation (9) can then be used to obtain a value for the friction factor (f) which is used as input to the Salter code.

Estimating values for diffuser efficiency in this case can be done by examining the curves given by Quinn in reference b showing $\Delta q/q_{IDEAL}$ as a function of diffuser half angle for the various ejector configurations tested. These values can then be related to an overall loss parameter q, i.e.,

$$q = q_{IDEAL} \left(1 + \Delta q/q_{IDEAL}\right) \tag{17}$$

where

$$q_{IDEAL} = 1 + (A_2/A_3)^2 . \tag{18}$$

Having computed a q for a given configuration and diffuser area ratio and previously having estimated values for θ_2 and ξ_f, a value for diffuser efficiency (η_D) can be obtained from the following expression, used by Quinn for his losses downstream of the injection plane.

$$q = 2\beta_2 \left(\xi_f + 1\right) - \eta_D \left[1 - (A_2/A_3)^2\right] \tag{19}$$

where η_D has been defined as

$$\eta_D = (\beta_2 \bar{C}_p)/C'_p \tag{20}$$

Fanchar (reference r) also did some work with the ARL diffusers and indicated the range of diffuser efficiencies as a function of diffuser half angle. These results, however, are all for half angles greater than 9° and as a result are only for the stalled conditions. The extracted diffuser efficiencies for the ARL data is shown in Figure 2.12 along with the nominal values indicated by Fanchar.

Taking the specific values for diffuser efficiency and using them for the code computations gives good agreement, as expected, with the experimental results for augmentation ratio. (Figure 2.13 A&B). At the conceptual design stage, however, one would not have these specifics, although it could be assumed that the general levels and characteristics of diffuser efficiency could be achieved. For this reason a nominal or generalized curve for diffuser efficiency (with no separation) has been developed from this data (Figure 2.12). Determining, a priori, the point or half angle where separation will occur in a given diffuser is a difficult task. Although some empirical relationships have been developed for specific ejector designs (see, for example, reference a), in general this would be unknown. Since it is desired to operate the ejectors in a region where the diffusers are not stalled, the nominal curve for diffuser efficiency, with no separation, shown in Figure 2.12 will be used. This generalized curve will be applied to the Rockwell International configurations as well as the jet-diffuser configuration developed by the Flight Dynamics Research Corporation.

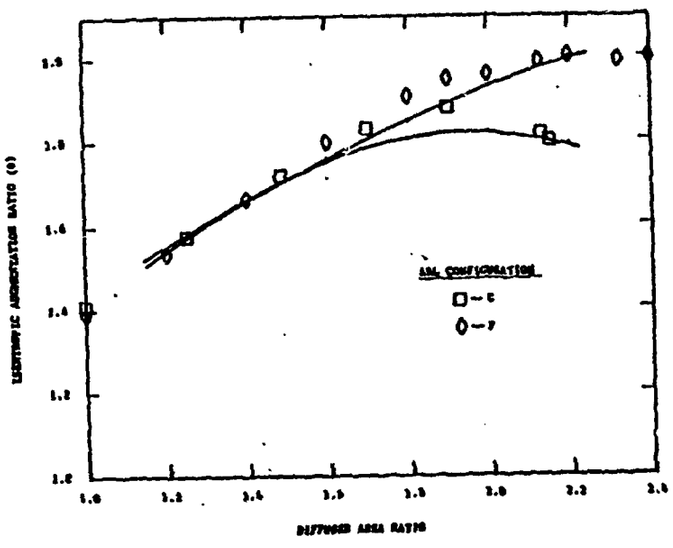

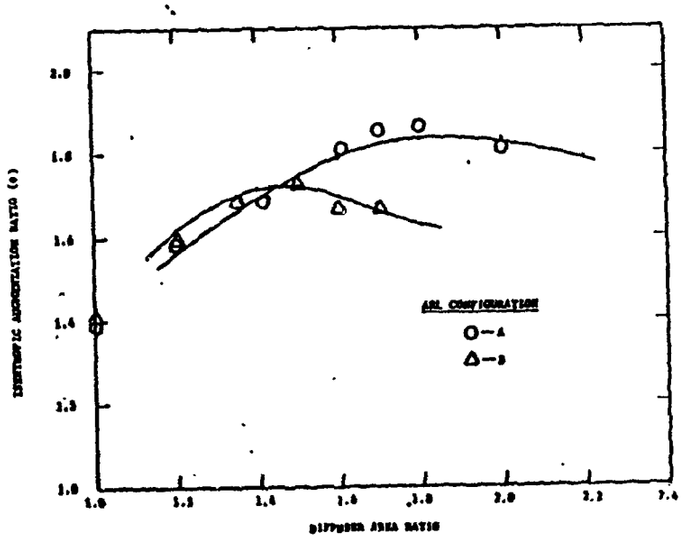

Figure 2.13 Comparison of Predicted and ARL Experimental Results.

2.3.2 Rockwell Configurations

In order to apply the simplified one-dimensional codes to the Rockwell International configuration, it requires that additional assumptions be made. These are primarily related to the inlet geometry. The generic Rockwell configuration is illustrated in Figure 2.14 and shows a centerbody with multiple nozzles that run along the span of the ejector. In addition to the centerbody, there are Coanda nozzles that are located on the inlet lips and generate wall jets along the diffuser flaps. These wall jets entrain secondary flow as well as provide a method of energizing the boundary layer in the diffuser and keep the flow attached. Unfortunately the weakest link in the diffuser is not the diffuser flaps but rather the end walls and corners. For this reason, small boundary layer control (BLC) nozzles (not shown) are provided to keep the flow in these critical areas attached.

For use in the one-dimensional codes, the centerbody, Coanda and BLC nozzles are all lumped into one primary nozzle located in the centerbody position. This is done, of course, on the basis of all primary and boundary layer control nozzles operating at the same pressure and temperature ratios. In addition, it will be assumed that the sum of the geometric primary and secondary flow area will be equal to the throat area of the ejector. This assumption is made because of the difficulty in considering multiple injection ports and trying to reference all flow areas to a common reference plane where the static pressure is assumed to be equalized. The length of the mixing section will be assumed equivalent to the running length, along the shroud, from the exit of the Coanda nozzles to the start of the diffuser section (or throat) of the ejector and will be assumed to be of constant cross-sectional area.

It was desired to know how useful the one-dimensional codes would be in estimating ejector performance with these simplifying assumptions. Two cases in particular were examined. The first configuration is a small scale ejector used by Rockwell to study corner separation (reference a). The second is the wing ejector that was developed for the XFV-12A technology demonstrator aircraft. Both of these ejectors are similar in cross-section to that shown in Figure 2.14. The small scale model, however, was a rectangular ejector whereas the XFV-12A wing was much more complex, having a tapered throat, tapered nozzles over the wing span and tapered flaps on the diffuser trailing edge. In order to simplify these configurations to something tractable and capable of being analyzed with these simplified codes, both ejectors will be idealized to the configuration as previously described. In the case of the XFV-12A ejector, average values at three separate locations along the span were used to provide a first order estimate of performance.

The centerbody used in the small scale model extended the length of the ejector span and consisted of 15 cross-slot nozzles. The specific details of this configuration are given in reference a. Some of the basic parameters of interest, however, are as follows:

Model Span----------1.667 ft (0.508m)

Throat Area/Total Nozzle Area ----------20.5

Mixing Section Length----------0.051 ft (0.0155m)

Diffuser Length----------0.584 ft (0.178m)

Total Nozzle Area----------0.033 ft^2 (0.00307m^2)

Nozzle Pressure Ratio----------1.5

Primary Gas Temperature----------540°R (300°K)

The mixing section length for friction losses in this case was assumed to be equal to the running length of the Coanda surface from the exit of the nozzle to the throat or start of the diffuser section.

The loss parameters to be assumed for this configuration are as follows:

Inlet loss parameters (ξ_1)----------0.025

Primary nozzle efficiency (η_N)----------0.90

Friction factor (f)----------0.250

Mixing effectiveness estimated at exit of diffuser (β_3)----------1.05-1.10

Diffuser efficiency (η_D)----------0.91-0.97

The inlet loss parameter has been assumed to be the same as the ARL configurations, since no better information is available. The primary nozzle efficiency is known to be somewhat less than the hypermixing nozzles and in this case will be assumed to be 0.90. The friction factor used is based on a reference velocity of 800 ft/sec (244 m/sec) which was the measured value of the Coanda wall jet given in reference a. Not having this information available, however, a reasonable first order estimate could be obtained by assuming the ejector to be ideal and using the computed primary stream velocity as a value for the reference velocity. The skewness factor at the exit of the diffuser has been assumed to be 1.05-1.10. Although there is no direct experimental evidence for these values given in reference a, similar laboratory models at Rockwell using hypermixing centerbody nozzles have given skewness values in this range.

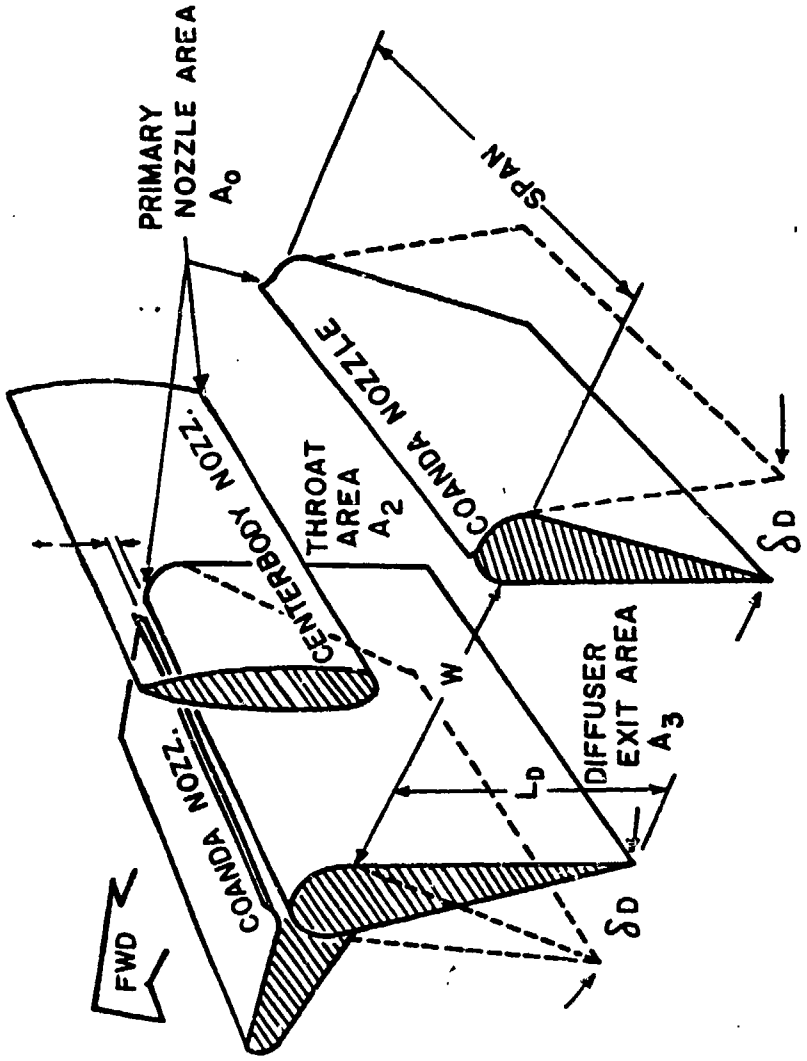

Figure 2.14 Generic Rockwell International Ejector Configuration

For this particular configuration, i.e., a cross-slot centerbody it is very difficult to determine if the diffusion process is in or perpendicular to the plane of the velocity profile. A cut through the center of the ejector at the span mid-point would see the peaks caused by two Coanda wall jets and the centerbody. Similarly a cut along the ejector span would see the velocity peaks of the individual cross slot nozzles. Since this point is not clear and the diffusion process could be considered in either mode it will be assumed in this case that $\beta_2 = \beta_3$.

Diffuser efficiency will again be considered to be a function of the diffuser half angle (δ_D). Since no better information is available, however, the diffuser efficiency will be assumed to follow the nominal curve shown in Figure 2.12. In this case the efficiency will be assumed to increase monotonically with the diffuser half angle to a value of 0.97 and a stall condition will not be assumed.

The results of these computations in comparison to experimental data are illustrated in Figure 2.15. In addition, the ideal curve (i.e., no losses) is also shown. It can be seen from these curves that better agreement with experimental data might have been achieved by varying skewness with diffuser half angle.

A similar analysis has been done for the XFV-12A wing configuration. Because of the detailed complexity of the ejector, numerous assumptions have to be made in order to make use of the simplified one-dimensional codes. Based on detailed configuration measurements at the wing root, mid span and tip, a nominal cross-section can be developed. Here again all the centerbody, Coanda and boundary layer control nozzles have been lumped together into a single primary centerbody nozzle. Some of the basic parameters of interest for this configuration are as follows:

Span----------8.956 ft (2.729m)

Throat area/Total Nozzle area----------16.0

Mixer length----------0.568 ft (0.277m)

Diffuser length----------3.02 ft (0.989m)

Total nozzle area----------0.8959 ft^2 (0.083m^2)

Nozzle pressure ratio----------2.3

Primary gas temperature----------1360°R (755°K)

The mixing section length in this case was again taken as the running length of the Coanda surface from the nozzle exit to the throat of the ejector.

The loss parameters assumed for this configuration are given as follows:

Inlet loss parameter (ξ_1)----------0.025

Primary nozzle efficiency (η_N)----------0.930

Friction Factor (f)----------0.223

Mixing effectiveness estimated at exit of diffuser (β_3)----------1.05-1.15

Diffuser efficiency (η_D)----------0.89-0.97

As in the small scale model previously discussed the inlet loss parameter will be assumed to be the same as measured by ARL. The primary nozzle efficiency will be assumed to be slightly less than that measured for hypermixing nozzles by ARL. The friction factor is based on a reference velocity of 1584 ft/sec (483 m/s) which is the sonic velocity for a nozzle flow at a total temperature of 1360°R and a pressure ratio based on the static pressure within the ejector at the inlet.

A range of skewness values at the exit of the diffuser are examined. These are based on values measured by Rockwell with the full scale model (not the aircraft hardware) and are quite typical for their configuration. It will also be noted that the diffusion process is primarily in the plane of the velocity profile and, therefore, the skewness at the end of the mixing section will be computed from equation (14).

Diffuser efficiency will again be considered to follow the nominal efficiency curve and will be assumed to monotonically increase (i.e., diffuser stall will not be considered) to a maximum value of 0.97 as was done for the small scale model (See Figure 2.12). The results of these estimates are shown in Figure 2.16 and compared to some initial full scale data taken by Rockwell on their whirl test rig (Ref. s).

In addition to the one-dimensional code, the 2-D finite difference code developed by Rockwell to analyze their particular configuration (i.e., a centerbody with two Coanda wall jets) was exercised. The code as it exists at present can only be applied to a centerbody that has hypermixing or slot nozzles. This is true because the empirical constants that have to be set within the input for the mixing analysis have only been established for these two types of nozzles. For this reason the code was not exercised for the small scale cross-slot centerbody ejector previously discussed. When used for the XFV-12A wing configuration, however, reasonably good estimates were obtained and are shown on Figure 2.16. These values tend to be a bit high, however, since only friction losses, mixing losses and primary nozzle losses are included. Inlet losses and diffuser efficiency values are not included in the analysis. In addition, the primary total temperatures were assumed to be somewhat lower (1260°R) than the values used for the one dimensional analysis because of difficulties in running the analysis. This also would tend to give a higher value for augmentation ratio.

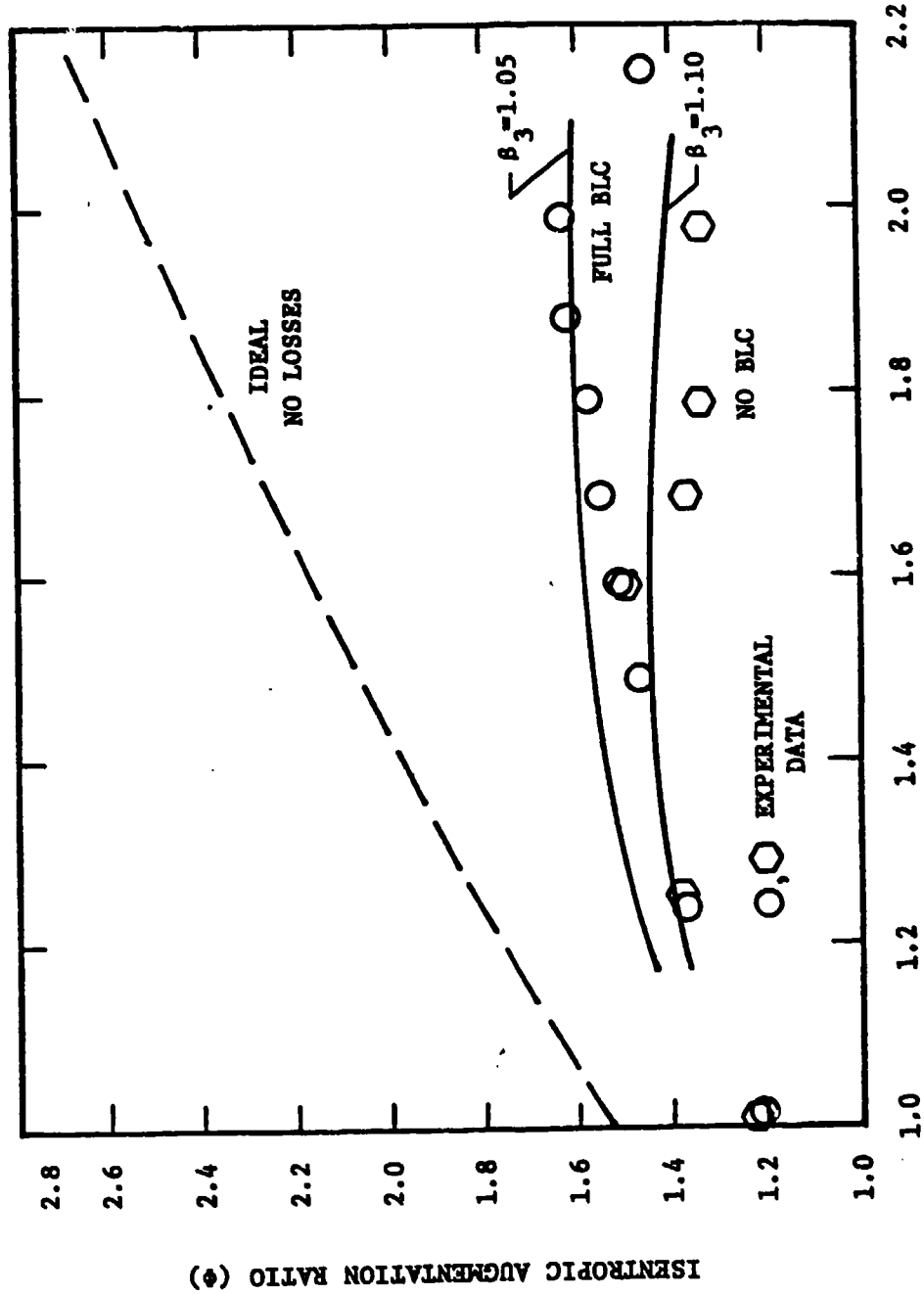

Figure 2.15 Comparison of Predicted and Experimental Data for Rockwell Configuration with Cross Slot Centerbody and Coanda Wall Jets.

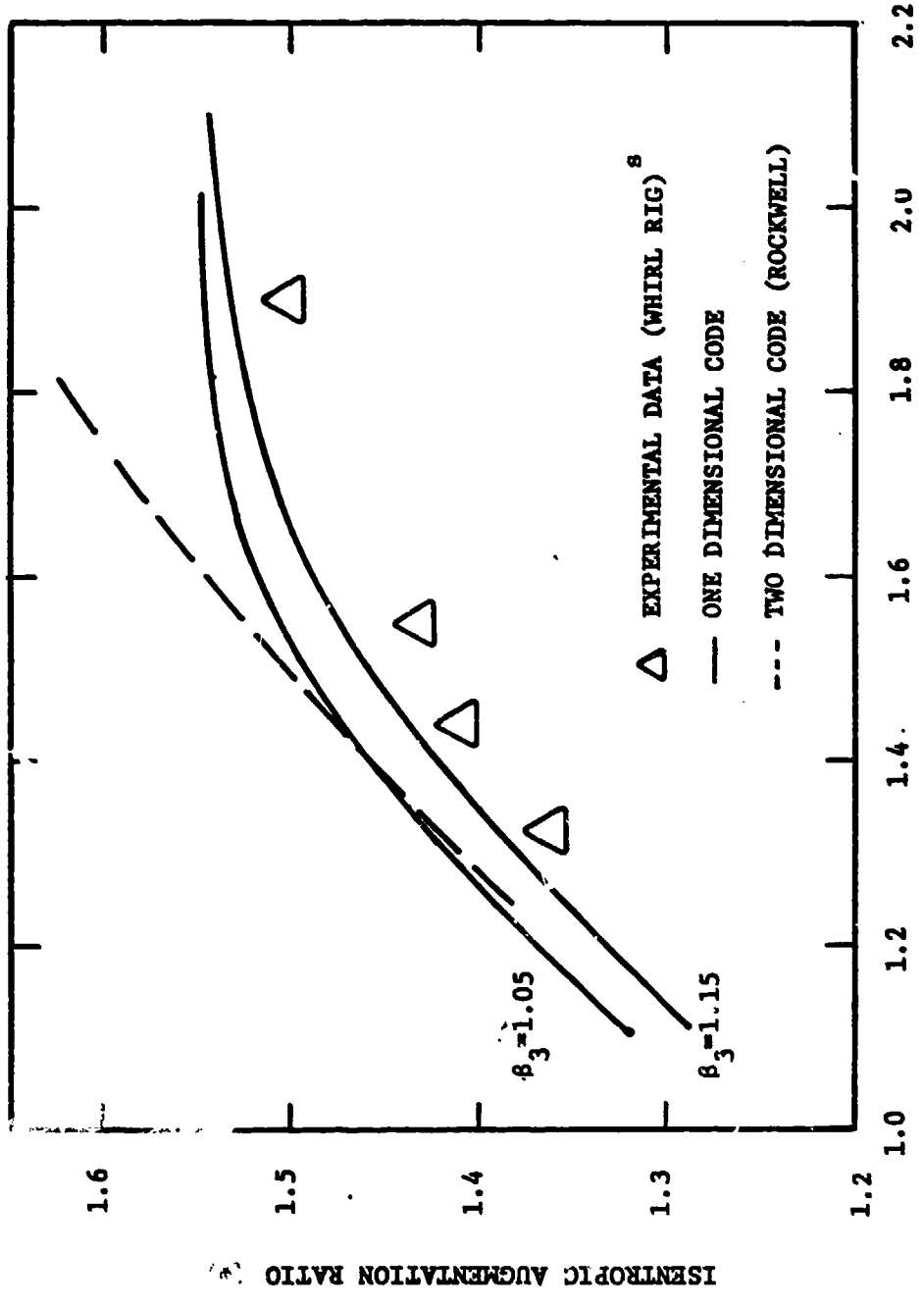

Figure 2.16 Comparison of Predicted and Experimental Data for Rockwell Full Scale Model of XFV-12A Wing.

2.3.3 Alperin Jet-Diffuser Ejector

The jet-diffuser concept for thrust augmentation was originally outlined by Morel and Lissaman (reference (t)). The specific jet-diffuser ejector discussed in this report was developed by the Flight Dynamics Research Corporation and has generated rather high augmentation ratios with a relatively short diffuser. The key to its high performance is the high velocity jet located around the throat of the ejector at the start of the diffuser section. This jet flow not only energizes the boundary layer to keep the diffuser flow attached at large diffuser half angles (up to 60°) but also allows the diffusion process to continue beyond the physical walls of the diffuser and, as a result, produces very high effective diffuser area ratios. The ejector herein discussed is known as the Alperin jet-diffuser ejector, was developed for the Navy's "Small Tactical Aerial Mobility Platform" program and is described in some detail in reference (d). A three view drawing of the ejector is shown in Figure 2.17.

In order to analyze this configuration the existing one-dimensional compressible code was modified to account for the jet-diffuser effect (that is, an effective diffuser area ratio that was greater than the physical diffuser) and the fact that this required an additional mass flow from a gas generator that was not being augmented as were the main primary flows.

The solution technique is to assume an initial effective diffuser area ratio that is 1.5 times that of the geometric diffuser area ratio. The entire ejector solution is then carried out with the assumption that the ejector flow to atmospheric pressure at the exit of the effective jet-diffuser and not the exit of the geometric diffuser. Once this has been done and all the flow and velocity parameters are now known, a value for the effective diffuser area ratio can be computed following a standard jet flap analysis illustrated in reference (m). If this value does not agree with the originally assumed value to within a specified tolerance, a new estimate for the effective diffuser area ratio will be made and the process repeated until the two values converge to within the given tolerance. Once the convergence condition is realized, all of the output values are printed.

The gross thrust of the ejector is now the augmented thrust of the primary nozzles plus the thrust from the diffuser jets minus losses to wall friction within the geometric diffuser. The isentropic nozzle thrust (needed to compute the augmentation ratio) now includes both the primary and diffuser nozzle flows expanding to ambient pressure. As in the previous analysis for the Rockwell configurations, the sum of the geometric primary nozzle area and the secondary flow area are considered to be equal to the ejector throat area.

Detailed experimental data has been taken on a jet-diffuser ejector built by the Flight Dynamics Research Corporation for the Navy. (Reference (u)). Based on this specific configuration, the modified one-dimensional ejector code has been run and the computed results compared to the experimental data. Some of the basic parameters of interest for this ejector are as follows:

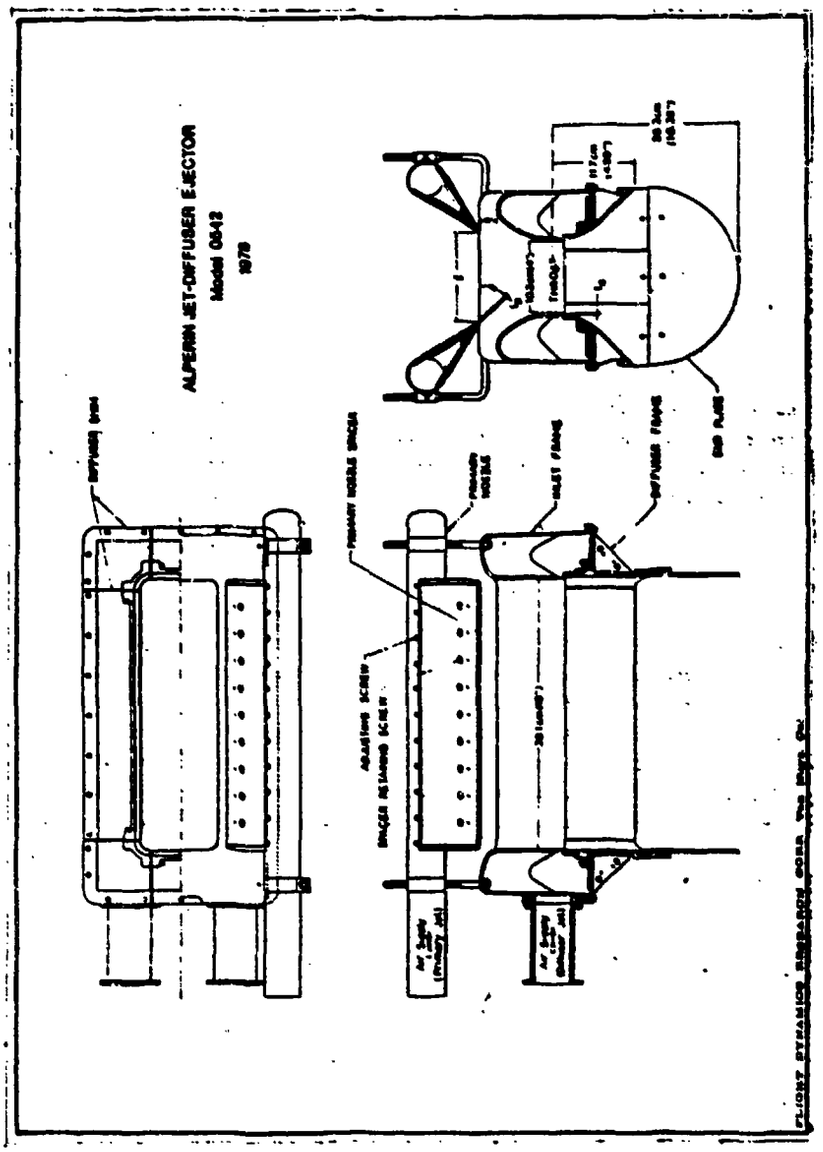

Figure 2.17 Alperin Jet Diffuser Ejector, "STAMP" Configuration.

Model Span----------1.25 ft (0.381m)

Throat Area/Primary Nozzle Area----------29.55

Mixing Section Length----------0.3199 ft(0.0975m)

Diffuser Wall Length----------0.4181 ft (0.127m)

Primary Nozzle Area----------0.0141 ft^2 ($0.0013m^2$)

Diffuser Nozzle Area----------0.0067 ft^2 ($6.22 \times 10^{-4} m$)

Geometric Diffuser Area Ratio----------2.5

Diffuser Surface Area----------1.6 ft^2 ($0.149m^2$)

The mixing section length in this case was again assumed to be equal to the running length of the inlet surface to the throat of the ejector. The diffuser wall length is the running length of the diffuser wall from the jet exit to the geometric end of the diffuser. For the most part, the primary and diffuser pressures and temperatures are maintained equivalent, although they were varied somewhat experimentally and could be varied independently in the modified code.

The loss parameters that have been assumed for this configuration are as follows:

Inlet Loss Parameter (ξ_1)----------0.0140

Primary Nozzle Efficiency (η_{NP})----------0.98

Diffuser Nozzle Efficiency (η_{ND})----------0.98

Friction Factor (f)----------0.0197

Mixing Effectiveness estimated at exit of effective diffuser (β_3)-------1.05

Diffuser Efficiency (η_D)----------0.98

The value for the inlet loss parameter was selected on the basis of experimental data on this configuration given in reference m. The primary nozzle efficiency was based on the smooth converging nozzle configuration used in this design. Since no better data was available, the same value was used for the diffuser nozzle. The friction factor is based on the turbulent flat plate skin friction coefficient which in turn is based on the average velocity at the ejector throat and the running length from

the inlet to the throat. The skewness at the exit of the effective diffuser was estimated on the basis of the experimental work provided by reference u. Since this diffusion process is in the plane of the velocity profile, equation (14) will be used to calculate the skewness at the exit of the mixing section. Based on this realtionship, it will be seen that the skewness values at the ejector throat are very low. This, coupled with the high effective diffuser area ratios, provides the reason for the excellent performance from the ejector. Diffuser efficiency is quite high and is based on the nominal curve shown in Figure 2.12. For this configuration the diffuser half angle is 45°.

A comparison of predicted and experimental values for augmentation ratio as a function of nozzle pressure ratio and temperature are shown in Figure 2.18. Rather good agreement has been obtained over a wide range of pressure ratios with the primary flow at ambient temperature. It can be seen that the augmentation ratio is essentially constant at the lower nozzle pressure ratios and falls off gradually as the pressure ratio increases. At higher temperatures (860°R) significant deviation between computed and experimental values occurs with the predicted value being lower than the actual data. A possible explanation for this difference comes from two areas. The first involves the fact that the primary exhaust total temperature was not actually measured and the temperatures reported experimentally are plenum temperatures. Substantial heat loss could have occurred within the primary nozzles causing the primary exhaust temperatures to be well below the plenum temperatures. Reducing the exhaust temperatures of the primary would cause an increase in the computed values for augmentation ratio. Secondly, experimental measurements have shown that the primary and diffuser areas increased slightly due to thermal expansion. This again supports the idea of high thermal losses from the primary flow. The increase in areas would also cause the computed values for augmentation ratio to increase slightly.

Excellent agreement has been obtained between experiment and theory for a number of parameters at the ambient temperature condition. These are illustrated in Table II and are based on nozzle pressure ratios of 1.31. and nozzle temperatures of $T_{t_N} = T_{t_D} = 520°R$ (288°K).

Table II
COMPARISON OF MEASURED AND COMPUTED
VALUES FOR "STAMP" EJECTOR (REF. u)

Parameter	Measured	Computed
Ejector gross thrust	47.609	47.882
Isentropic nozzle thrust	26.004	26.194
Augmentation ratio	1.8308	1.828
Primary nozzle mass flow rate	0.8172	0.8382
Diffuser mass flow rate	0.4108	0.3974

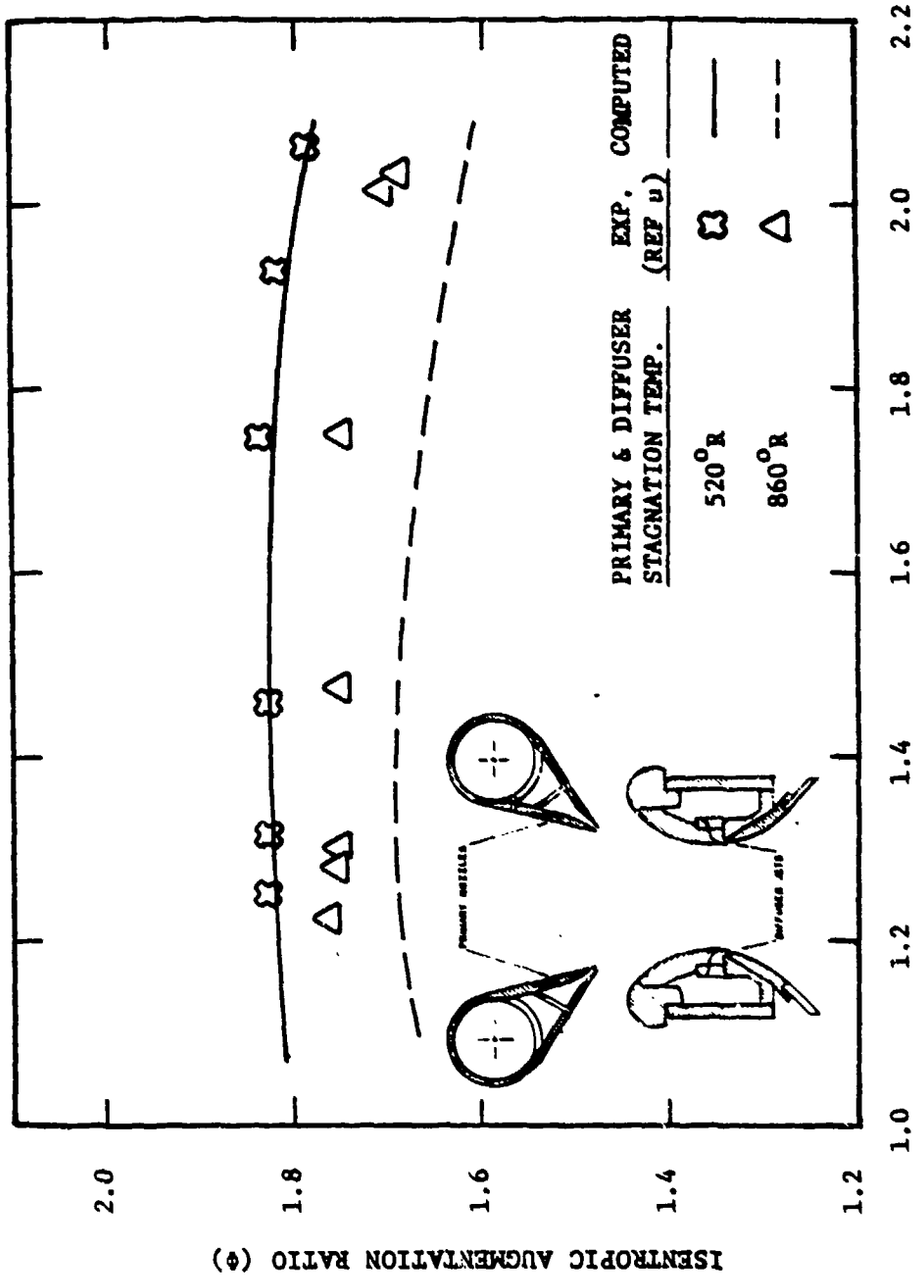

Figure 2.18 Comparison of Predicted and Experimental Data for Alperin Jet-Diffuser Ejector, "STAMP" Configuration.

3.0 Conclusions

The usefulness of the complex two and three dimensional mixing codes for ejector analysis, at this point, appear to have only limited application. This is particularly true if one is at the conceptual design stage and many of the detailed parameters and constants required for these codes are not available. Once these codes are properly "tuned" i.e., the constants required in the mixing analysis are properly set, very useful parametric studies on the detailed flows can be accomplished. These computer runs can, however, be rather long and expensive depending upon the complexity of the problem and the detail desired in the output.

The simplified one-dimensional codes, particularly the analysis developed by Salter and modified at the NAVAIRDEVCEN, appear to be very useful at the conceptual and preliminary design stage. Despite some of the assumptions that have to be made to simplify the configurations and the loss parameters that must be estimated, reasonable agreement can be obtained with experimental data. The most sensitive of these assumptions appear to be the extent of mixing (characterized by flow skewness) and the diffuser efficiency.

Modifications to the original Salter code have allowed performance estimates to be made of a jet-diffuser type ejector with good agreement with experimental results.

In addition to computing overall performance, estimates can be made of the primary and diffuser mass flow that would be required from the gas generator, the secondary inlet mass flows and velocities as well as the ejector exit mass flows and velocities. All this information, of course, would be required by a designer when considering the overall aerodynamic performance of an aircraft.

4.0 References

a. Seiler, M. R., "An Investigation of Corner Separation Within a Thrust Augmenter Having Coanda Jets", NAVAIRDEVCEN Report 76153-30, 1977.

b. Quinn, B. "Recent Developments in Large Area Ratio Thrust Augmenters", AIAA Paper No. 72-1174.

c. O'Donnell, R. M., Squyers, R. A., "V/STOL Ejector Short Diffuser Study", NAVAIRDEVCEN Report 77165-30, 1976.

d. Alperin, M., Wu, J. J., "The Alperin Jet-Diffuser Ejector (AJDE) Development, Testing and Performance Verification Report", NAVWEPCEN Report TP 5853, 1976.

e. Viets, H., "Thrust Augmenting Ejectors", ARL Report 75-02224, 1975.

f. Bevilaqua, P. M., "Evaluation of Hypermixing for Thrust Augmenting Ejectors", Journal of Aircraft, Vol. 11, No. 6, 1974.

g. Salter, G. R., "A Computer Program for Aircraft Thrust Ejector Analysis", AIAA Paper No. 74-1191, 1974.

h. Gilbert, G. B., & Hill, P. G. "Analysis and Testing of Two-Dimensional Slot Nozzle Ejectors with Variable Area Mixing Sections", NASA CR 2251, 1973.

i. Rushmore, W. L., Zelazny, S. W. "A Three Dimensional Turbulent Compressible Flow Model for Ejector and Fluted Mixers", NASA CR-159467, 1978.

j. von Karman, T., "Theoretical Remarks on Thrust Augmentation", Reissner Anniversary Volume, Edwards Bros, Ann Arbor, Mich., 1949, pp. 461-468.

k. Bevilaqua, P. M., De Joode, A. D., "Viscid/Inviscid Interaction Analysis of Thrust Augmenting Ejectors", ONR CR212-249-1, 1978.

l. Alperin, M., Wu, J. J., "High Speed Ejectors", Sponsored by Air Force Flight Dynamics Laboratory, Under Contract No. F33615-77-C-3160, Report No. AFFDL-TR-79-3048.

m. Alerpin, M., Wu, J. J., "Underwater Jet-Diffuser Ejector Propulsion-Real Fluid Effects", Flight Dynamics Research Corporation Report 0294-8-78, Sponsored by the Office of Naval Research under Contract No. N00014-77-C-0294, 1978.

n. Quinn, B., "The Decay of Highly Skewed Flows in Ducts", Journal of Engineering for Power, January 1975.

o. Viets, H., Quinn, B., "Concurrent Mixing and Diffusion in Three Dimensions," AIAA Paper No. 75-873.

p. Viets, H., "Directional Effects in 3-D Diffuser", AIAA Journal Vol. 13, No. 1, January 1976.

q. Bevilaqua, P. M., "Analytic Description of Hypermixing and Test of an Improved Nozzle", Journal of Aircraft Vol. 13, No. 1, January 1976.

r. Fanchar, R. B., "Low Area Ratio, Thrust Augmenting Ejector", Journal of Aircraft, Vol. 9, No. 3, March 1972, pp. 243-248.

s. Rockwell International Corporation Technical Review on XFV-12A, 25 July 1978.

t. Morel, J. P., and Lissaman, P. B. S., "The Jet Flap Diffuser: A New Thrust Augmenting Device," AIAA Paper No. 69-777, 1969.

u. Dejneka, R., Naval Air Propulsion Center, Private Communication.

5.0 List of Symbols

A	Area
BLC	Boundary Layer Control
C_D	External nozzle drag coefficient
C_f	Skin friction coefficient
$\overline{C_p}$	Diffuser pressure coefficient
C_V	Nozzle velocity coefficient
D_h	Hydraulic diameter
f	Friction factor
h	Ejector span
K_1	Inlet loss coefficient
L_D	Diffuser length
L_m	Mixing section length
$\dot{m}$	Mass flux
NPR	Nozzle pressure ratio
NTR	Nozzle temperature ratio
p	Static pressure
P	Pressure
q	Term for ejector losses, downstream from plane of injection
$\Delta q/q$	Measure of duct-diffuser losses
T	Thrust or Temperature
v	Velocity at a point
$\overline{V}$	Mass average velocity
V_N'	Isentropic nozzle velocity
w	Width of ejector throat

β	Flow skewness or momentum coefficient
δ_D	Diffuser half angle
η_D	Diffuser efficiency
η_e	Energy transfer efficiency
η_N	Nozzle efficiency
ν	Kinematic viscosity
ξ_1	Inlet loss parameter
ξ_f	Friction coefficient
ρ	Density
ϕ	Augmentation Ratio

Subscripts

0,1,2,3	Station Positions
a	Atmospheric or Ambient Conditions
D	Diffuser or Drag
f	Friction
G	Gross
i	Isentropic
m	Mixing
N	Net or Nozzle
p	Primary
ref	Reference
s	Secondary or Surface
t	Total or Stagnation Conditions

Distribution List
Report No. NADC-80094-60

AIRTASK NO. A03V/0000/001B/9F41-400-000

	No. of Copies
NAVAIRSYSCOM (AIR-950D)	5
(2 for retention)	
(1 for AIR-320D:D. Kirkpatrick)	
(1 for AIR-330:R. Brown)	
(1 for AIR-330B:E. Lichtman)	
NAVAIRPROPCEN	2
(1 for PE42:A. Atkinson)	
(1 for PE63:R. Dejneka)	
Office of Naval Research, Arlington, Virginia	1
(1 for Dr. R. Whitehead)	
DTIC	12